sustainability

MDPI

Article

Agroforestry Optimisation for Climate Policy: Mapping Silvopastoral Carbon Sequestration Trade-Offs in the Mediterranean

Diogenis A. Kiziridis, Ilias Karmiris and Dimitrios Fotakis *

Forest Research Institute, Hellenic Agricultural Organization DIMITRA, 57006 Thessaloniki, Greece; danis.k@zoho.com (D.A.K.); iliask@elgo.gr (I.K.)
* Correspondence: fotakis@elgo.gr

Abstract

Effective implementation of silvopastoralism, a key Nature-Based Solution for Europe's climate goals, is hindered by a lack of decision-support tools clarifying trade-offs between efficiency and extent of carbon sequestration. To address this, we developed a multi-objective scenario analysis (4064 scenarios) to identify optimal strategies for silvopastoral expansion across the EU27 Mediterranean bioregion. We found an inverse relationship defining a clear trade-off: scenarios achieving the highest mean sequestration (up to 2.5 Mg CO_2 ha^{-1} $year^{-1}$) are spatially limited, whereas those maximising total gains (approaching 10^7 Mg CO_2 $year^{-1}$ in total) do so by incorporating vast areas, lowering mean rates. This trade-off is formalised by a Pareto front, from which we defined a best-balanced optimal scenario and three policy regimes (conservative, balanced, expansive). Progressing across the front involved shifting from converting primarily shrubby and sparsely vegetated lands to incorporating grasslands and mixed agro-systems. At the NUTS2 level, Spain and Greece emerged as hotspots. Notably, converting arable land was not a primary contributor to carbon gains, as the marginal carbon benefit on these productive soils is lower than on marginal lands due to their higher baseline soil carbon levels, indicating that large-scale implementation can focus on marginal lands to avoid conflicts with food security. While subject to uncertainties of the underlying land-use and carbon models, this analysis demonstrates that our framework enables policymakers to select spatially explicit strategies aligned with specific budget or sequestration goals. These insights can inform CAP eco-schemes and national LULUCF strategies. The resulting maps and code are freely available.

Keywords: silvopasture; agroforestry; optimisation; carbon; sequestration; Pareto; Mediterranean; land use; modelling; policy

Academic Editor: Pablo Peri

Received: 3 November 2025
Revised: 23 December 2025
Accepted: 30 December 2025
Published: 1 January 2026

1. Introduction

The escalating climate crisis has placed land-based carbon sequestration at the heart of EU decarbonisation policy through frameworks like the European Green Deal and LULUCF Regulation [1–4]. Translating these high-level commitments into concrete land-use strategies, however, remains a central challenge, requiring a balance between climate, biodiversity, and socio-economic objectives [5,6].

Silvopastoral agroforestry is a Nature-Based Solution with exceptional potential to contribute to this balance, enhancing carbon stocks, soil health, and biodiversity [7–13].

Despite this multifunctionality, it remains underrepresented in European landscapes and policy [14,15], though emerging instruments like the CAP eco-schemes now recognise its value [16]. The effective implementation of such policy instruments requires spatially explicit evidence on where such systems are most feasible and beneficial.

Policymakers and stakeholders increasingly demand decision-support tools capable of identifying priority areas, quantifying potential gains, and assessing trade-offs under diverse environmental and management conditions [17]. A critical requirement for such tools, especially in the context of constrained budgets and competing land-use objectives, is the ability to transparently map the trade-offs between maximising per-hectare sequestration efficiency and maximising total sequestration extent across a landscape. However, evidence for agroforestry has identified a persistent research gap in tools that generate spatially explicit, trade-off-aware guidance for policy implementation [18]. Existing spatial models for land-based carbon mitigation often focus on reforestation, afforestation, or soil carbon enhancement under single-objective criteria [19,20]. Although valuable, these approaches tend to overlook the multifunctionality of agroforestry systems and the socio-ecological variability across Europe. Moreover, they frequently provide static outputs, identifying a single "optimal" map, without accounting for the multiple, often competing objectives that underpin policy decisions [21]. This is a critical methodological shortfall, as recent reviews confirm that while decision-support tools exist, they often fail to effectively integrate the competing socio-economic and ecological objectives inherent to real-world land-use planning or to produce a set of alternative optimal solutions that reflect different policy priorities [22,23].

Recent advances in multi-criteria and multi-objective spatial optimisation have opened new opportunities for overcoming these limitations. Tools such as Marxan, Zonation, and spatially explicit Pareto front analyses have been widely adopted for conservation planning, renewable energy siting, and agricultural resource allocation [24–26]. These frameworks allow the explicit quantification of trade-offs between conflicting goals, such as maximising ecosystem service provision while minimising economic cost or land-use conflict. Despite this potential, applications of such optimisation approaches to agroforestry or silvopastoral planning remain rare and geographically limited. Most existing models operate at regional or national scales, focusing on discrete ecological objectives or policy-specific indicators rather than providing a transparent exploration of decision space [27–29]. Consequently, policymakers are often left with coarse or prescriptive recommendations that cannot easily be adapted to differing regional priorities or constraints.

The Mediterranean bioregion provides a particularly compelling context for applying these advanced spatial tools. Characterised by steep climatic gradients, recurrent droughts, and centuries-long anthropogenic transformation, Mediterranean landscapes are inherently complex mosaics of cropland, shrubland, and woodland [30,31]. Many of these areas face acute land degradation, declining soil fertility, and depopulation of rural communities [32–34]. Yet, this same heterogeneity provides an ecological and socio-economic foundation for adaptive land-use systems such as silvopastoralism. Traditional Mediterranean practices—such as the Spanish dehesa and Portuguese montado—exemplify the long-standing coexistence of productive use and ecological stewardship, sustaining both biodiversity and cultural heritage [35,36]. Recent continental-scale analysis confirms that these and related systems are central to Europe's agroforestry carbon sink, with silvopastoral areas predominantly clustered in this bioregion [37]. These systems demonstrate that tree–livestock integration can thrive even under semi-arid conditions, provided that management is locally adapted and supported by enabling policies. However, outside the Iberian Peninsula, such models have not been systematically assessed. Widespread adoption is also challenged by structural socio-economic constraints common to Mediter-

ranean rural areas, such as an ageing farmer population, low farm profitability, and land fragmentation [38]. Furthermore, recent stakeholder analyses highlight that silvopastoralism in Mediterranean regions continues to face significant policy and economic barriers, including a framework perceived as ineffective and issues of low competitiveness [38], leaving considerable uncertainty about where and how silvopastoral expansion could best contribute to the EU's climate and land restoration goals [39,40].

A key challenge lies in developing analytical tools that can capture the intrinsic trade-offs between efficiency and extent in land-based mitigation strategies. For example, prioritising the highest sequestration efficiency per hectare may favour small, isolated patches of high productivity, while maximising the total area of intervention could lead to broader, but less carbon-dense, outcomes [29,41,42]. Identifying this continuum of possible strategies, and understanding where the balance between them lies, is essential for informed, context-sensitive policymaking. Furthermore, such analyses must consider both the biophysical potential of land and the practical realities of agricultural systems, including land availability, existing land uses, and local socio-economic conditions [43].

This study aimed to answer the following research questions: (1) What is the spatial trade-off frontier (Pareto front) between the mean carbon sequestration per hectare and the total carbon sequestration potential for silvopastoral expansion in the Mediterranean bioregion? (2) How can this frontier be partitioned into distinct, policy-relevant strategic regimes? (3) What key environmental and management thresholds (e.g., suitability, slope, livestock density) define the transition between these regimes? These questions extend earlier, more generic spatial optimisation by focusing explicitly on the policy-actionable outcomes for silvopastoral systems in the Mediterranean: the trade-off frontier, strategic regimes, and defining thresholds.

We addressed these questions by developing a spatially explicit, multi-objective optimisation framework that mapped the trade-off frontier for silvopastoral expansion across the Mediterranean bioregion of the EU27. Building on the foundations of spatial ecology, carbon modelling, and decision science, our approach generated a Pareto front of optimal scenarios that jointly maximised (i) sequestration efficiency (mean carbon gain per hectare) and (ii) total sequestration potential (total area). By visualising the continuum between these competing objectives, we identified distinct strategic regimes corresponding to alternative policy preferences. In doing so, this work quantifies the spatial potential of silvopastoralism as a land-based mitigation pathway, and provides a flexible, evidence-based decision-support framework for scaling up agroforestry measures in alignment with European climate, land-use, and carbon neutrality objectives.

2. Materials and Methods

This study quantified the potential carbon sequestration gains from the hypothetical adoption of silvopastoral practices across the Mediterranean bioregion of the European Union (EU27). Our methodology was based on a high-resolution, spatially explicit simulation framework (Figure 1). We first established a baseline of current land cover and associated carbon stocks. We then projected plausible land cover transitions reflecting pro-silvopastoral land management. The carbon sequestration potential was estimated by quantifying changes in three primary pools from the baseline to the projection of taking measures for silvopastoralism: vegetation biomass, soil organic carbon (SOC), and livestock-mediated soil carbon inputs. Finally, we conducted a comprehensive scenario analysis of prioritising high-potential Areas Of Interest (AOI) for agroforestry implementation under varying biophysical and policy constraints, culminating in the identification of an optimal trade-off between sequestration efficiency and land area commitment to silvopastoralism management. Analyses were performed at a spatial resolution of 1 km^2 (100 ha per grid

cell) in the European ETRS89-LAEA (EPSG:3035) projection, to harmonise datasets, and to facilitate regional aggregation at the NUTS-2 level. All spatial analyses were performed in version 4.1.2 of the R programming environment [44], using the terra package for raster data manipulation [45], and the tidyterra and ggplot2 packages for visualisation [46,47].

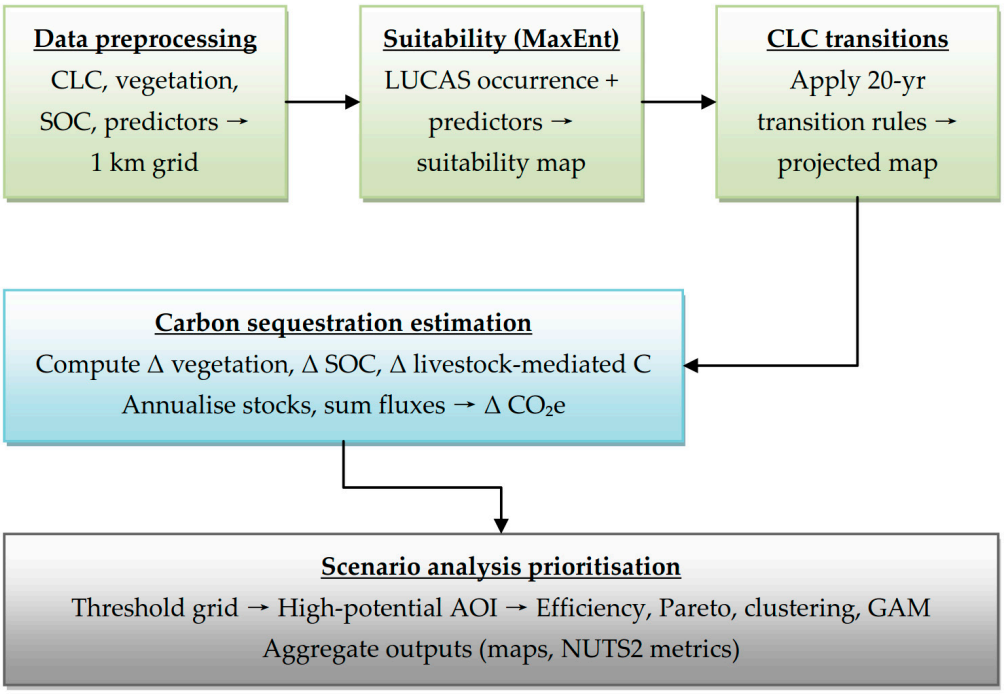

Figure 1. Simplified workflow of our silvopastoral carbon simulation, from data harmonisation and suitability modelling to carbon estimation, scenario analysis, and final spatial outputs. Abbreviations: SOC stands for Soil Organic Carbon; AOI stands for Area Of Interest; and GAM stands for Generalized Additive Model.

2.1. Study Region and Baseline Land Cover

To define the study region's baseline extent of lands suitable for silvopastoral systems (Figure 1), we identified a set of "eligible" CORINE Land Cover (CLC) classes [48], which were in any terrestrial region within the EU27 classified under the Mediterranean biogeographical region [49]. The total coverage of the study region was approximately 817,680 km^2. The foundational land cover data was derived from the CORINE Land Cover (CLC) 2018 dataset [50], resampled from its native 100 m resolution to 1 km pixel dimension (Figure 2).

The eligible CLC classes included agricultural, semi-natural, and forest landscapes where silvopastoralism is either currently practiced, or could be feasibly introduced. The primary eligible classes were (class code): Pastures (231), Complex cultivation patterns (242), Land principally occupied by agriculture, with significant areas of natural vegetation (243), Agro-forestry areas (244), Natural grasslands (321), Sclerophyllous vegetation (323), Transitional woodland-shrub (324), Broad-leaved forest (311), Coniferous forest (312), and Mixed forest (313).

The selection was expanded to include Non-irrigated arable land (211), Vineyards (221), Fruit trees and berry plantations (222), Olive groves (223), Moors and heathland (322), and Sparsely vegetated areas (333). The final baseline land cover raster was created by masking the CLC map to retain only pixels belonging to the 16 entirely eligible classes.

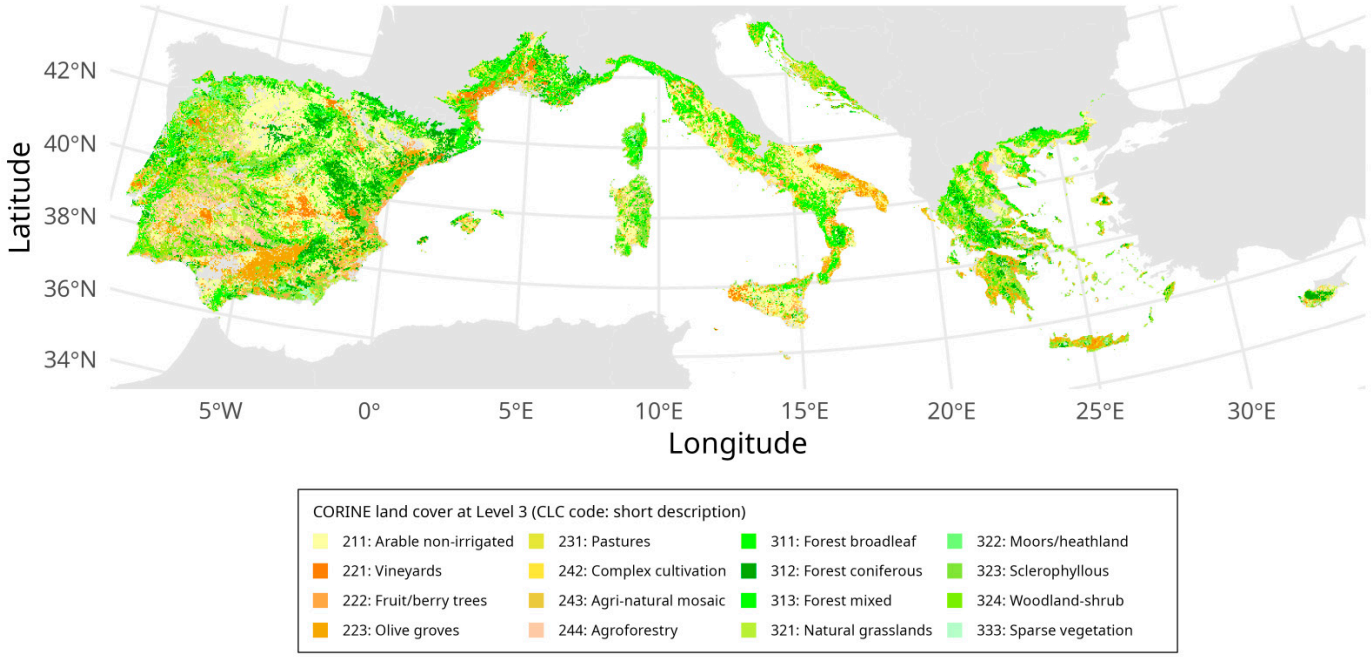

Figure 2. Baseline land cover and study region. Extent and distribution of CORINE Land Cover (CLC) classes eligible for silvopastoralism within the Mediterranean bioregion of the EU27. Map uses the official CLC palette, focusing on the overall distribution. Raster resolution: 1 km.

These 16 classes were selected because they represent established or potential silvopastoral systems where tree-livestock integration is ecologically plausible, economically viable without major structural changes, and aligns with current landowner capacities. We excluded wetlands, urban areas, and intensive croplands. Exclusions were based on ecological unsuitability (e.g., wetland hydrology), prohibitive conversion costs, or high conflict with existing intensive land uses, making silvopastoral introduction infeasible.

The CLC classes were grouped into 10 land cover groups based on functional and structural similarity (e.g., all forest types, all shrublands), primarily to facilitate the visualisation and interpretation of results (Table 1). The percent cover of the 10 land cover groups in the study region's NUTS2 regions (Nomenclature of Territorial Units for Statistics Level 2) is provided in Table S1.

Table 1. Grouping the 16 eligible CLC classes into 10 land cover groups to facilitate visualisation.

Land Cover Group	CLC Code, Name (% Baseline Cover)
Agroforestry	244, Agroforestry (4.3%)
Arable land	211, Arable non-irrigated (21.2%)
Forest	311, Broadleaf (13.2%); 312, Coniferous (7.8%); 313, Mixed (3.7%)
Grasslands	321, Natural grasslands (5.8%)
Mixed agro-systems	242, Complex cultivation (5.3%); 243, Agri-natural mosaic (4.8%)
Pastures	231, Pastures (1.7%)
Shrubby vegetation	322, Moors/heathland (1.5%); 323, Sclerophyllous (11.5%)
Sparsely vegetated	333, Sparse vegetation (1.3%)
Tree plantations	221, Vineyards (3%); 222, Fruit/berry (2.3%); 223, Olive groves (6%)
Woodland-shrub	324, Woodland-shrub (6.6%)

2.2. Silvopastoralism Suitability Modelling

To identify areas with high potential for silvopastoralism, we developed a species distribution model (SDM), using the Maxent algorithm [51]. This approach models the environmental suitability for silvopastoral systems based on a set of known occurrence

points, and a comprehensive suite of environmental and socioeconomic predictors [28]. The resulting continuous suitability map (ranging from 0 to 1) served as a key input for the subsequent scenario analysis.

2.2.1. Silvopastoralism Occurrence Data

Occurrence data for existing silvopastoral systems were derived from the 2022 Land Use and Cover Area frame Survey (LUCAS), a harmonised in situ survey conducted across the EU [52]. We developed a classification scheme based on the LUCAS microdata fields [53], focusing on the columns for primary land cover (`SURVEY_LC1`, `SURVEY_LC1_SPEC`) and observed grazing (`SURVEY_GRAZING`).

A LUCAS point was classified as "silvopastoral" if it met two criteria: (1) visible signs of grazing were recorded, and (2) the primary land cover was a woody type, including woodlands (codes starting with 'C'), shrubland with sparse trees ('D10'), or permanent woody crops like fruit trees and olive groves (codes 'B7' and 'B8'). Given the focus of this study, only the 4426 points classified as silvopastoral and located within the EU27 Mediterranean bioregion were retained for modelling (Figure S1c).

Background data are required for Maxent modelling [51]. To minimise sampling bias inherent in presence-only datasets, we employed a "target-group background" approach [54]. The background points were randomly sampled (n = 20,000) from all LUCAS points within the study region that were not classified as silvopastoral (Figure S1a,b). This ensures that the background data share the same geographic and methodological biases as the presence data, leading to a more robust model.

The classification of LUCAS points as silvopastoral is based on harmonised field observations and is considered the best available continental-scale data for this purpose [55]. However, some degree of misclassification is possible, for example, if grazing was temporary or if tree cover was misrecorded. To mitigate the impact of such potential errors on the model, we used a spatially structured validation approach (block cross-validation) and a target-group background, both of which reduce the influence of spatial and sampling biases that could arise from classification inaccuracies.

2.2.2. Ecological and Socioeconomic Predictors

All predictors were processed to a common 1 km spatial resolution and aligned to the ETRS89-LAEA (EPSG:3035) projection. Data gaps within the study region were filled using a focal median (for continuous data) or focal modal (for categorical data) filter with an 11 × 11 moving window, followed by a global mean/modal fallback to ensure complete coverage.

A total of 14 predictor variables were compiled to represent the climatic, topographic, soil, and socioeconomic conditions influencing silvopastoral suitability (Table 2):

- Land cover: A CLC 2018 raster [48], aggregated to 1 km using a modal function (Figure S2), was included as a categorical predictor to capture the influence of the surrounding landscape matrix.
- Bioclimatic variables: Four variables were sourced from the WorldClim 2.1 dataset [56]: annual mean temperature (BIO1), temperature seasonality (standard deviation × 100, BIO4), annual precipitation (BIO12), and precipitation seasonality (coefficient of variation in percentage, BIO15). These were processed from their native 30 s resolution, reprojected, resampled to the 1 km grid, and finally classified to ordinal levels (Figure S3).
- Topographic variables: Elevation, aspect, and slope were derived from the Copernicus Digital Elevation Model (DEM) over Europe (EU-DEM) [57], aggregated to 1 km.

Elevation and slope were classified into five ordinal levels, and aspect was categorised into eight cardinal directions (Figure S4).

- Soil properties: Three topsoil (0–30 cm) variables were obtained from the European Soil Database (ESDB) of the JRC [58]: total organic carbon content (TOC), total available water content (TAWC), and soil texture class (TTEXT). These were reclassified into ordinal levels, or categories based on their original documentation, and resampled to the 1 km grid (Figure S5).
- Socioeconomic variables: Three NUTS3-level indicators for the year 2022 were sourced from Eurostat: median population age [59], population density [60], and employment rate for ages 15–64, i.e., percentage of the population in the 15–64 year range [61] that is employed [62]. These vector-based data were rasterized to the 1 km grid. Missing values were imputed using the mean of neighbouring NUTS3 regions, with a country-level median as a fallback (Figure S6).

Table 2. Predictor variables used in the MaxEnt silvopastoralism suitability model.

Predictor	Resolution	Rationale	Source
Land cover (categorical)	1 km (modal aggregation)	Represents dominant landscape context affecting grazing and tree cover	CLC 2018 [48]
Annual mean temperature (BIO1)	1 km (from 30″)	Captures climate suitability for woody vegetation and livestock	WorldClim 2.1 [56]
Temperature seasonality (BIO4)	1 km (from 30″)	Reflects climatic extremes influencing vegetation and forage stability	WorldClim 2.1 [56]
Annual precipitation (BIO12)	1 km (from 30″)	Indicates water availability for biomass productivity	WorldClim 2.1 [56]
Precipitation seasonality (BIO15)	1 km (from 30″)	Represents drought stress risk affecting grazing capacity	WorldClim 2.1 [56]
Elevation	1 km (aggregated)	Topographic constraint shaping vegetation structure and microclimate	EU-DEM [57]
Slope	1 km (aggregated)	Limits accessibility for livestock and mechanised management	EU-DEM [57]
Aspect	1 km (categorised)	Influences solar radiation and vegetation patterns	EU-DEM [57]
Topsoil organic carbon (TOC)	1 km (reclassified)	Indicator of soil fertility and biomass retention potential	ESDB [58]
Topsoil available water content (TAWC)	1 km (reclassified)	Determines vegetation resilience under grazing pressure	ESDB [58]
Soil texture class (TTEXT)	1 km (categorical)	Affects root penetration, water retention and tree establishment	ESDB [58]
Median population age	1 km (rasterised)	Proxy for demographic structure influencing labour availability	Eurostat (2022) [59]
Population density	1 km (rasterised)	Indicates human pressure and land-use competition	Eurostat (2022) [60]
Employment rate (ages 15–64)	1 km (rasterised)	Represents socio-economic conditions supporting farming	Eurostat (2022) [61,62]

Multicollinearity among the predictors was assessed using Spearman's rank correlation and Generalized Variance Inflation Factors (GVIFs) calculated from the presence

and the background point data. All absolute pairwise correlations were below 0.7, and all GVIFs were below 2.98, confirming acceptable independence for MaxEnt modelling.

2.2.3. MaxEnt Model Implementation and Selection

We used the ENMeval R package to tune and evaluate a set of candidate MaxEnt models [63]. ENMeval systematically tests different combinations of feature classes (FC) and regularization multiplier (RM) values to identify the optimal model configuration. We tested three feature class combinations (Linear-Quadratic 'LQ', Linear-Quadratic-Hinge 'LQH', and Hinge 'H') and a range of regularisation multipliers from 1 to 3 (in steps of 0.5).

Model performance was evaluated using spatial block cross-validation, which partitions the data into four geographic quadrants to account for spatial autocorrelation. Both occurrence and background data were partitioned into the same geographic blocks. This block method is robust to spatial sorting bias, and model performance was consistent across partitions, indicating low sensitivity to specific quadrant boundaries. The best model was selected based on the lowest Akaike Information Criterion corrected for small sample sizes (AICc), which balances model fit and complexity.

The optimal model (LQH features, RM = 2.0) achieved a test AUC of 0.736 with moderate overfitting (ΔAUCtrain-test = 0.044). While AUC values from presence-background models should be interpreted with caution as they are sensitive to the extent of background sampling, our model's validation AUC of 0.736 indicates moderate discriminatory ability, and is sufficient for regional policy prioritization, as it effectively identifies broad geographic patterns of silvopastoral potential rather than requiring pixel-specific prediction. Average omission rate at the 10% training presence threshold was 0.129. Permutation importance identified CLC as the strongest contributor (61.3%), followed by population density (11.6%) and precipitation seasonality (7.5%). Percent contribution was led by CLC (56.8%). Jackknife tests confirmed CLC provided the most unique information when used in isolation (training gain = 0.3045). This final, tuned model was then run on the full dataset (all presence and background points) to generate the final silvopastoralism suitability map for the entire study region (Figure S7).

In summary, we employed a presence-only MaxEnt model to map silvopastoralism suitability across the Mediterranean bioregion. Occurrence data (n = 4426) were extracted from the 2022 LUCAS survey, using a target-group background sampling approach. Fourteen climatic, topographic, soil, and socioeconomic predictors at 1 km resolution were compiled. Model selection identified optimal parameters (LQH features, regularization multiplier = 2.0), with spatial block cross-validation yielding a robust predictive performance. The resulting continuous suitability map served as a foundational spatial input for the subsequent scenario analysis.

2.3. Projection of Land Cover to Silvopastoralism Transition

We projected the baseline land cover in a 20-year horizon for simulating the potential impact of policies promoting the maintenance, expansion and intensification of agroforestry in general, and silvopastoralism in particular, in the study region. Our selection of a 20-year horizon aligns with the EU's 2030–2050 decarbonisation trajectory outlined in the European Green Deal [1], and the LULUCF Regulation [3], while providing sufficient time for measurable carbon stock changes—such as initial tree growth and soil organic carbon (SOC) accumulation—as recommended in IPCC AFOLU guidelines [5].

The land cover projection is based on a set of plausible transitions between the eligible CLC classes, informed by CLC nomenclature guidelines and ecological succession principles.

The core of these land cover changes involves the conversion of open agricultural and grassland systems to more integrated, wooded systems. Specifically, the following transitions were modelled, representing biophysically plausible pathways where socio-economic conditions (e.g., farmer incentives, market shifts) could enable adoption:

1. Non-irrigated arable land (211), Vineyards (221), Fruit trees (222), Olive groves (223), Pastures (231), Complex cultivation (242), Agri-natural mosaic (243), and Natural grasslands (321) were transitioned to Agroforestry (244).
2. Sclerophyllous vegetation (323), Moors and heathland (322), and Sparsely vegetated areas (333) were transitioned to Transitional woodland-shrub (324).

Classes that already represent stable silvopastoral or forested systems were assumed to remain unchanged. These include existing Agroforestry (244), Transitional woodland-shrub (324), and all forest classes (311, Broad-leaved; 312, Coniferous; and 313, Mixed forest). This conservative assumption reflects that transitions of established forests are generally restricted under EU policy.

The modelled transition and persistence resulted in the land cover change of the baseline with the 10 land cover groups to the projection with only three groups: Agroforestry, Forest, and Woodland-shrub (Figure 3).

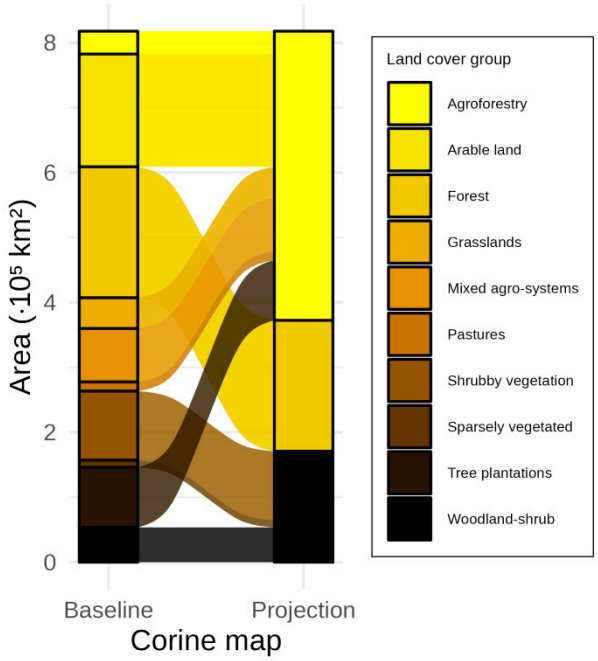

Figure 3. Land cover groups and transitions in the study region for the assumed 20-year period. Bars indicate the area of each land cover group, and flows from baseline to projection depict the transitions.

The transition rules were applied to the baseline land cover raster using a reclassification matrix to generate the map of projected land cover. Figure 4 illustrates the baseline and projection maps of land cover groups in the study region.

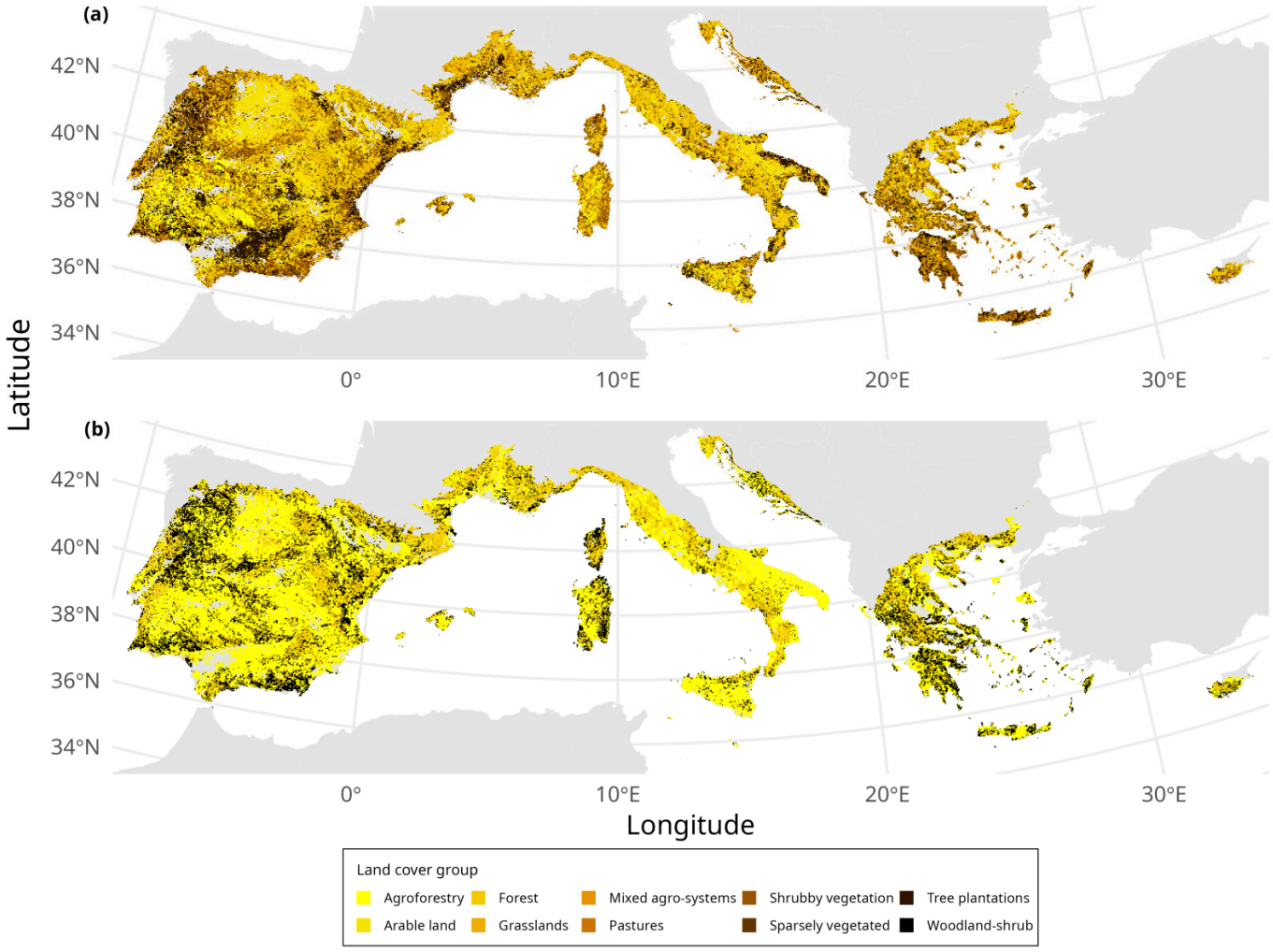

Figure 4. Land cover groups in the study region: (**a**) baseline based on Corine 2018 land cover; (**b**) projection assuming policies for enhancing silvopastoralism in a 20-year horizon. Raster resolution: 1 km.

2.4. Carbon Sequestration Modelling

The total change in carbon sequestration was calculated as the sum of changes across three key components over a 20-year time horizon:

1. Above- and below-ground vegetation carbon stock.
2. Soil organic carbon (SOC) stock.
3. Livestock-mediated carbon sequestration from manure deposition.

Changes in vegetation and SOC stocks were amortised over the 20-year period to yield an annual rate, (*projection* − *baseline*)/20, while the livestock component was modelled as a direct annual flux, consistent with IPCC Tier 2 accounting methodologies [64].

The three components were modelled independently (additively), without simulating biogeochemical feedbacks between them, consistent with a Tier 2 accounting approach. The central assumption for the vegetation and SOC projections is that, over 20 years, transitioned land will develop carbon stocks analogous to existing, stable systems of the target land cover class under similar environmental conditions.

All carbon stock and flux values were ultimately converted to CO_2 equivalents (CO_2e) using a conversion factor of 3.67 (i.e., the molar mass ratio of CO_2/C) [65].

2.4.1. Vegetation Carbon Stock

The baseline vegetation carbon stock was derived from the Global Vegetation Carbon Stock dataset for the year 2020 (units: Mg C ha^{-1}), which provides data at a 300 m resolution [66]. The global raster was cropped to the buffered extent of the study region, reprojected to the EPSG:3035 coordinate system, and resampled to the 1 km analysis grid using bilinear interpolation. The resulting raster was masked to the eligible land cover extent. Any remaining data gaps within the study region were filled using a focal median function with an 11 × 11 moving window (Figure S8a).

To estimate the projection of vegetation carbon stock in a 20-year horizon, we developed a k-Nearest Neighbours (k-NN) imputation model. This approach estimates the carbon stock for a transitioned pixel by borrowing values from existing, persistent in their land cover pixels that share similar characteristics. Specifically, for each pixel undergoing a land-cover transition, we identified the $k = 10$ nearest spatial neighbours that already existed in the target land cover class under baseline conditions and shared the same levels of environmental characteristics in: annual mean temperature (Figure S3a), total precipitation (Figure S3c), elevation levels (Figure S4a), and slope (Figure S4c). The new carbon value was imputed as the mean of these neighbours' baseline carbon stocks. A nested fallback logic was implemented to handle cases with insufficient neighbours:

1. Primary: Mean of 10 nearest neighbours with the same target land cover and environmental group.
2. Fallback 1: Mean of fewer than 10 nearest neighbours with the same target land cover and environmental group (at least one neighbour required).
3. Fallback 2: Mean of 10 nearest neighbours with only the same target land cover.
4. Fallback 3: Mean of 10 nearest neighbours with only the same levels of environmental conditions.
5. Fallback 4: If no analogues are found, the pixel retains its baseline carbon value.

Finally, to ensure the projection only represented carbon gains, the final imputed values for transitioned pixels were clamped to be no less than their baseline values (Figure S8b).

2.4.2. Soil Organic Carbon (SOC) Stock

Baseline SOC stock (0–30 cm depth) was obtained from the SoilGrids 2.0 dataset at 250 m resolution (units: Mg C ha^{-1}) [67]. The dataset was processed following the same workflow as for vegetation carbon: reprojection to EPSG:3035, resampling to 1 km, masking to the study region, and gap-filling using a focal median filter (Figure S10a). SOC stock for the projection after 20 year was estimated using the same k-NN imputation methodology described for vegetation carbon, using topsoil texture category instead of slope level in the set of environmental predictors: annual mean temperature (Figure S3a), total precipitation (Figure S3c), elevation levels (Figure S4a), and topsoil texture (Figure S5c). To reduce the influence of artefactual extreme values, SOC values greater than 212 Mg C ha^{-1} (approximate maximum expected from the SoilGrids web map) were clamped. Finally, projection SOC values were similarly clamped to be greater than or equal to baseline values (Figure S10b).

2.4.3. Livestock-Mediated Carbon Sequestration

The contribution of livestock to soil carbon sequestration was estimated using a streamlined mass-balance model applied per livestock unit (LSU) [64]. This model calculates the net amount of carbon returned to the soil via manure after accounting for all major carbon outflows from the animal system. The model was parameterised separately for cattle and for a combined sheep and goats category. The final sequestration rate in Mg C ha^{-1} $year^{-1}$ was derived by multiplying the per-animal sequestration by the LSU density (LSU ha^{-1}).

Baseline LSU density for cattle (grazing and seminatural) and for sheep/goats (seminatural) was obtained at 100 m resolution [68], based on an integrated methodology combining agricultural and veterinary datasets with field observations, expert assessments, and machine-learning techniques to produce spatially explicit maps of grazing livestock distributions across the European Union [69]. The dataset was processed by resampling to 1 km, and masking to the study region (Figure S12).

The mass-balance calculation proceeds as follows for the baseline map (Figure S14a):

1. **Carbon Intake (C_{in})**: Annual carbon intake was calculated as the product of annual dry matter intake DMI_{annual} and the carbon content of forage dry matter $C_{content,DM}$ which was assumed to be 45% [70]:

$$C_{in} = DMI_{annual} \times C_{content,DM}. \quad (1)$$

DMI_{annual} was estimated as the percentage $DMI_{\%BW}$ of animal body weight BW_{kg}, using values of 2.5% for cattle [71] and 4.0% for sheep/goats [72]:

$$DMI_{annual} = BW_{kg} \times \frac{DMI_{\%BW}}{100} \times 365. \quad (2)$$

BW_{kg} was assumed to be 365 kg and 45 kg for cattle and sheep/goats, respectively [71,72].

2. **Carbon Outflows ($C_{out} = C_{products} + C_{respiration} + C_{methane}$)**: Carbon outflows were partitioned into the following pathways:
   - **Animal Products ($C_{products}$ from milk and growth):** Carbon exported in milk and new body tissue was subtracted. This was calculated using literature-derived values for annual milk yield assumed to be 3500 kg and 400 kg for, respectively, the cattle and sheep/goats [73,74], the carbon content of milk assumed to be 11% of its weight [75], annual body growth assumed to be approximately 65 kg and 123 kg for, respectively, and cattle and sheep/goats [76], and carbon content of body tissue assumed to be approximately 19% and 15% for respectively the cattle and sheep/goats [77].
   - **Respiration ($C_{respiration}$)**: Carbon lost as CO_2 through maintenance respiration was estimated. We first calculated the maintenance energy requirement scaled by metabolic body weight ($BW^{0.75}$), relative to a reference weight for expressing results per LSU (650 kg) [78]. This maintenance energy (MJ day^{-1}) was converted to CO_2 production using a fixed energy-to-CO_2 factor (0.07 kg CO_2 MJ^{-1}) [79]. The carbon percent of DMI (45%) provided the ingested carbon, while 27.3% of CO_2 mass corresponds to carbon [80]. The resulting carbon respired, and percentage of ingested carbon lost as CO_2, quantify respiration-related carbon turnover per animal.
   - **Methane Emissions ($C_{methane}$)**: Carbon lost as methane (CH_4) from enteric fermentation and manure management was assumed to be 87 kg CH_4 LSU^{-1} year^{-1} and 8 kg CH_4 LSU^{-1} year^{-1} for cattle and sheep/goats, respectively [64]. The mass of methane was converted to the mass of carbon using the molar mass ratio of carbon to methane (12/16).
3. **Net Manure Carbon Input (C_{manure})**: The carbon remaining for deposition as manure was calculated as the residual of intake minus all outflows:

$$C_{manure} = C_{in} - C_{\text{out}} = C_{in} - \left(C_{products} + C_{respiration} + C_{methane}\right) \quad (3)$$

4. **Final Sequestered Carbon ($C_{sequestered,LSU}$)**: The amount of manure carbon that becomes stabilised in the soil was estimated by applying a sequestration efficiency coefficient (η_{seq}) to the net manure C input. This coefficient represents the fraction of deposited carbon that is incorporated into long-term SOC pools. Based on meta-analyses of manure application studies, we used efficiency values of 15% for cattle [81], and 30% for sheep/goats [82]. The model assumes uniform manure deposition and does not account for non-linear density effects such as soil compaction:

$$C_{sequestered,LSU} = C_{manure} \times \eta_{seq} \quad (4)$$

For the projection of livestock-mediated sequestration rates we imputed using the same k-NN methodology applied to vegetation and SOC, ensuring that sequestration rates in transitioned pixels were analogous to those in structurally similar, established landscapes (Figure S14b).

Parameter uncertainty was estimated through the mass-balance model assuming moderate uncertainty levels: body weight (±10%), dry matter intake (±15%), milk yield (±15%), growth rate (±20%), methane emissions (±25%), and sequestration efficiency (±15%). We estimated an asymmetric 90% confidence interval [0.0453, 0.1178] Mg C ha^{-1} year^{-1}, which reflects the log-normal nature of biological distributions. Uncertainty in livestock-mediated carbon sequestration was quantified via Monte Carlo simulation (n = 100). The resulting 95% confidence interval for total sequestration was [0.0430, 0.1218] Mg C ha^{-1} year^{-1} around the mean estimate of 0.0786 Mg C ha^{-1} year^{-1}, representing a coefficient of variation of 27.1%. Cattle contributions accounted for 93.6% of the total variance, with sequestration efficiency coefficients and dry matter intake rates identified as the dominant sources of uncertainty. This level of uncertainty (±27%) is comparable to other land-based carbon accounting studies and reflects the inherent variability in livestock production systems and soil carbon dynamics [83].

2.5. Scenario Analysis Framework for Identifying High-Potential Areas

To move beyond a single, static projection, we developed a scenario analysis framework to explore a wide parameter space, and identify AOI with high potential for silvopasture under different assumptions. A "high-potential" pixel was defined as one that satisfied a combination of five filtering thresholds: it had a slope and suitability not lower than, respectively, the minimum slope and suitability thresholds, it had a tree cover and livestock density not higher than respectively the maximum tree cover and livestock density thresholds, and it was not included under a land protection regime. We created a parameter grid by systematically varying the thresholds for these criteria, resulting in 4064 unique scenarios.

The filtering thresholds for including a pixel as high-potential were the following:

1. Minimum slope: We tested thresholds of 1°, 3°, 5°, 7°, 10°, 15°, and 20°. Pixel slope was given from the continuous version of the slope raster (Figure S4c).
2. Minimum silvopastoralism suitability: We tested thresholds from 0.3 to 0.9 with a 0.1 increment. This threshold was based on the map of predicted suitability from the previously developed MaxEnt SDM (Figure S7).
3. Maximum tree cover density: Thresholds ranged from 10% to 60% with a 10% increment. Tree cover density for the study area was derived from 2021 GLOBMAP Fractional Tree Cover tiles [84]. We applied a mosaicking of all MODIS sinusoidal tiles intersecting the area of interest, reprojecting the mosaic to the EPSG:3035 grid, and resampling it to 1 km resolution. Remaining data gaps were filled using an 11 × 11 median focal filter and global mean fallback (Figure S16).

4. Maximum livestock density: We tested thresholds 0.01, 0.05, 0.1, 0.2, 0.4, 0.6, and 1.0 LSU ha^{-1} from the baseline map of LSU density (summing the LSU densities from cattle and sheep/goats in Figure S12a,b, respectively).
5. Land protection status (strict versus relaxed): We hypothesised two protection regimes: strict versus relaxed. Initially, a protected areas map was created by merging the Natura 2000 sites (Birds and Habitats Directives; types B and C) [85], and the CDDA national designations (IUCN Ia–III and equivalent strict conservation categories) [86]. Both datasets were reprojected to the EPSG:3035 grid, clipped to the study extent, simplified, and dissolved into a single exclusion mask that identifies zones that could be restricted from agroforestry or land-use modification (Figure S17). We defined two policy regimes regarding the protected areas:
    - Strict regime: All protected areas were excluded from consideration.
    - Relaxed regime: Protected areas were excluded unless they already supported grazing (LSU density greater than 0 LSU ha^{-1}), acknowledging that some forms of agriculture are permissible in certain designated areas.

The tested threshold ranges for slope, tree cover, and livestock density were designed to systematically target marginal agricultural and semi-natural landscapes, a recognised strategic priority for silvopastoral implementation. This "marginal lands first" approach focuses on areas with lower agronomic potential or existing pastoral use, where introducing trees and livestock adds ecosystem value with minimal socio-economic conflict, and aligns with documented strategies for scaling agroforestry [38,87,88].

For each of the 4064 scenarios, we generated a binary mask of high-potential AOI and calculated the total and mean carbon sequestration change across the identified area.

2.6. Statistical Analysis and Scenario Prioritisation

The outputs from the scenario analysis were used to understand the trade-offs and drivers of carbon sequestration potential.

First, we conducted a Pareto front analysis to identify the set of "Pareto-optimal" scenarios. In this context, a scenario is optimal if no other scenario exists that provides both a higher total sequestration and a higher mean sequestration per hectare. This allowed us to filter out suboptimal scenarios and focus on the direct trade-off between the scale and intensity of carbon gains.

Second, to identify a single "best-balanced" scenario among the Pareto-optimal set, we calculated an efficiency score for each optimal scenario, defined as the min–max normalised sum of the scaled total sequestration and scaled mean sequestration, penalised by the scaled land area required. We then located the "knee point" of the efficiency curve using a curvature-based method (with the uik function from the inflection R package [89]). This point represents the optimal trade-off, where the marginal gain in efficiency per unit of additional land begins to diminish significantly.

Third, to understand the underlying structure of the optimal solutions, we applied k-means clustering to the Pareto-optimal scenarios based on their threshold parameters and efficiency scores. This partitioned the Pareto front into three distinct policy-relevant "regimes" representing conservative, balanced, and expansive approaches to agroforestry implementation, respectively.

Fourth, to quantify the influence of each threshold parameter on sequestration efficiency, we fitted a Generalised Additive Model (GAM) using the mgcv package [90]. The efficiency score was modelled as a non-linear function of the four continuous threshold parameters and the categorical protection regime. All possible two-way interactions between the five predictor variables were systematically tested. Model selection via AIC identified the interaction between minimum suitability and minimum slope thresholds as the most

parsimonious. The partial effects from this best-fit GAM were used to interpret how each constraint influences the overall efficiency of the agroforestry transition.

Finally, to provide useful output at the administrative level, we focused on three metrics that were aggregated for each NUTS2 area of the study region: (a) the extent of high potential, as the inter-scenario mean percentage of each NUTS2 area's cover selected for measures; (b) the patchiness, or spatial heterogeneity of potential, quantified as the coefficient of variation (CV) of the selection frequency values of all pixels within each NUTS2 region; and (c) the mean total sequestration change, derived by averaging the total carbon gains per NUTS2 region across all scenarios. Moreover, we analysed the land cover composition of the high-potential AOI in the three scenarios representing the endpoints of the conservative, balanced, and expansive regimes on the Pareto front. For each NUTS2 area, we identified the single land cover group that accounted for the largest portion of that NUTS2 area's total sequestration gain. This "top contributor" was then mapped to visualise the geographic distribution and dominant landscape drivers of carbon gains under each of the three distinct policy-relevant strategies.

In summary, we identified optimal scenarios via Pareto front analysis, filtering for non-dominated solutions. A best-balanced scenario was selected using a min–max normalised efficiency metric, with the knee point identified subsequently. k-means clustering grouped optimal solutions into three policy-relevant regimes (conservative, balanced, expansive). GAMs quantified non-linear threshold influences on efficiency. Finally, we aggregated outcomes to NUTS2 regions, calculating extent, patchiness, mean sequestration, and identifying dominant land cover contributors across regimes.

3. Results

3.1. Carbon Stock Changes from Baseline to Projection

The transition from the baseline land cover to the pro-silvopastoral projection resulted in a net increase across all three modelled carbon pools, though the magnitude and distribution of these gains varied significantly (Figure 5). The total carbon stock in the study region's vegetation increased from a baseline mean of approximately 100 Mg CO_2 ha^{-1} to a projected mean of over 200 Mg CO_2 ha^{-1}, with the largest gains concentrated in areas transitioning to more wooded systems (Figure 5a). Similarly, the SOC stock showed a consistent, albeit less pronounced, increase across the region (Figure 5b). The most dynamic changes were observed in the livestock-mediated carbon sequestration potential, underscoring the critical, dual role of livestock in sustainable Mediterranean agroecosystems: providing livelihood security while contributing to soil health through the recycling of organic nutrients in manure. While many areas had negligible baseline values, the projection showed a substantial increase in potential carbon inputs from manure, particularly in newly established agroforestry and transitional woodland-shrub systems (Figure 5c). The mean total sequestration change due to vegetation, SOC, and livestock together was approximately 7 Mg CO_2 ha^{-1}, with a standard deviation of 13.42 Mg CO_2 ha^{-1} for vegetation, 3.66 Mg CO_2 ha^{-1} for SOC, and 0.05 Mg CO_2 ha^{-1} for livestock manure.

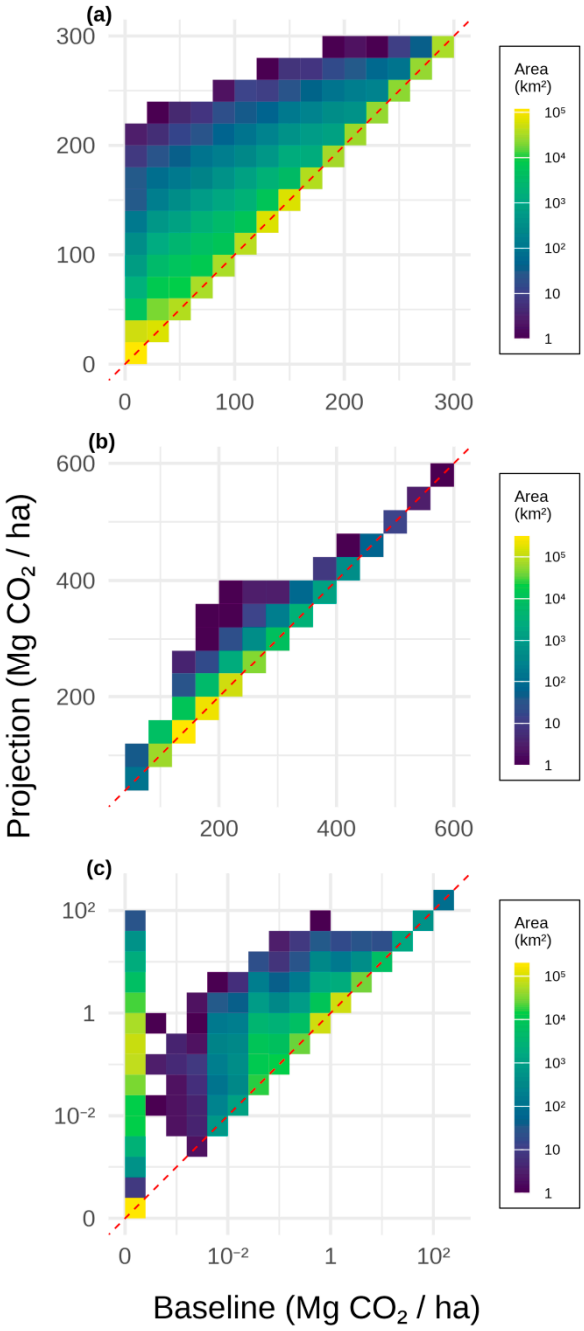

Figure 5. Baseline versus projection carbon stock, and the area they covered in the study region. The stocks are from the sum of: (**a**) vegetation carbon stock; (**b**) SOC stock; and (**c**) livestock-mediated carbon through manure.

3.2. Scenario Analysis and Identification of Optimal Strategies

The scenario analysis, comprising 4064 unique combinations of biophysical and policy constraints, revealed a clear trade-off between the mean sequestration rate per hectare, and the total sequestration achieved across the high-potential landscape. This relationship is demonstrated by the Pareto front, which algorithmically isolated the set of optimal scenarios where it is impossible to increase total sequestration without decreasing mean sequestration rate (Figure 6). From the 4064 simulated scenarios, the Pareto filter identified 40 non-dominated (optimal) points, defining the trade-off frontier.

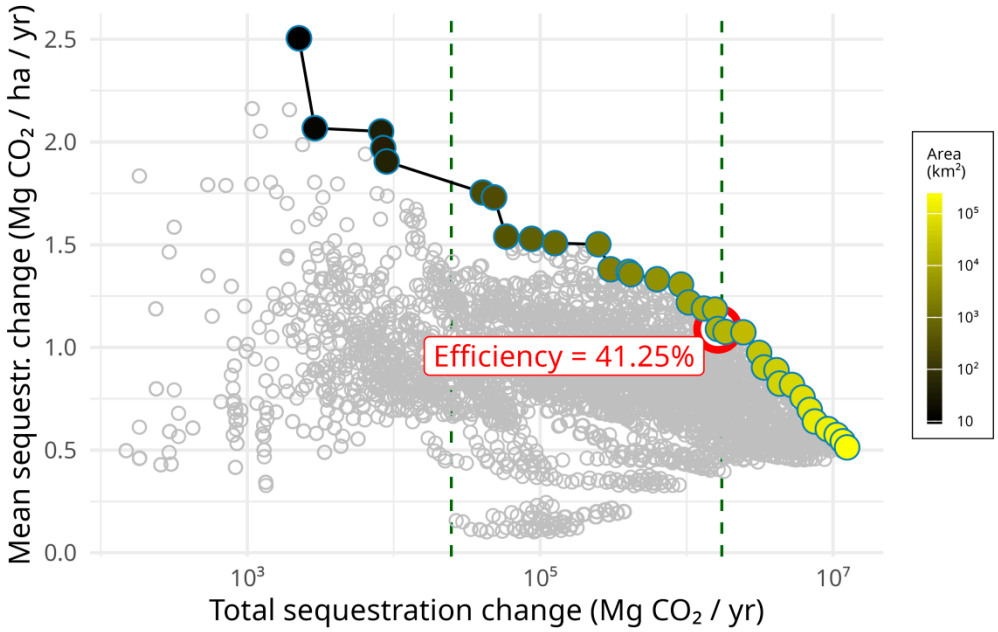

Figure 6. Pareto front along the mean versus total change in sequestration rates from the baseline to the 4064 high-potential AOI of the scenarios. The Pareto points are filled with the colour/shading of their area, according to the legend. The red circle indicates the optimal Pareto point, with the label indicating its efficiency. The dashed vertical lines divide the Pareto front in the three identified regimes.

The Pareto-optimal scenarios formed a distinct curve, showing that scenarios delivering the highest mean sequestration change (up to ~2.5 Mg CO_2 ha^{-1} $year^{-1}$) are limited to very small, highly suitable AOI. Conversely, scenarios achieving the highest total sequestration (approaching 10^7 Mg CO_2 $year^{-1}$) do so by incorporating vast land areas, which drives the mean sequestration rate down to ~0.5 Mg CO_2 ha^{-1} $year^{-1}$.

Using the min–max normalised efficiency metric that balances total gains, mean gains, and land area, we identified the optimal "knee point" of the Pareto front at an efficiency of 41.25% of its maximum value (indicated with the red circle in Figure 6). This optimal scenario, the 26th in the descending order of Pareto points, represents the best-balanced trade-off, capturing substantial carbon gains before the onset of significantly diminishing marginal returns in the AOI. Notably, the empirically derived knee point from the Pareto front—balancing total change, mean change, and area—did not exactly match the GAM maxima (Figure S18). This reflects that the GAM shows isolated effects assuming other predictors are typical, whereas the knee reflects trade-offs actually realised in the simulations.

The k-means clustering of the Pareto-optimal scenarios further partitioned the front into three distinct policy-relevant regimes: (1) a conservative regime of high mean gain, and low total area (Pareto points 1–9); (2) a balanced regime of moderate mean gain, and moderate total area (Pareto points 10–26); and (3) an expansive regime of low mean gain, and high total area (Pareto points 27–40).

3.3. Drivers of Sequestration Potential Along the Pareto Front

Analysis of the environmental and threshold variables along the 40 scenarios of the Pareto front reveals the shifting characteristics of high-potential AOI as the strategy moves from the conservative to the balanced and then to the expansive regime (Figure 7).

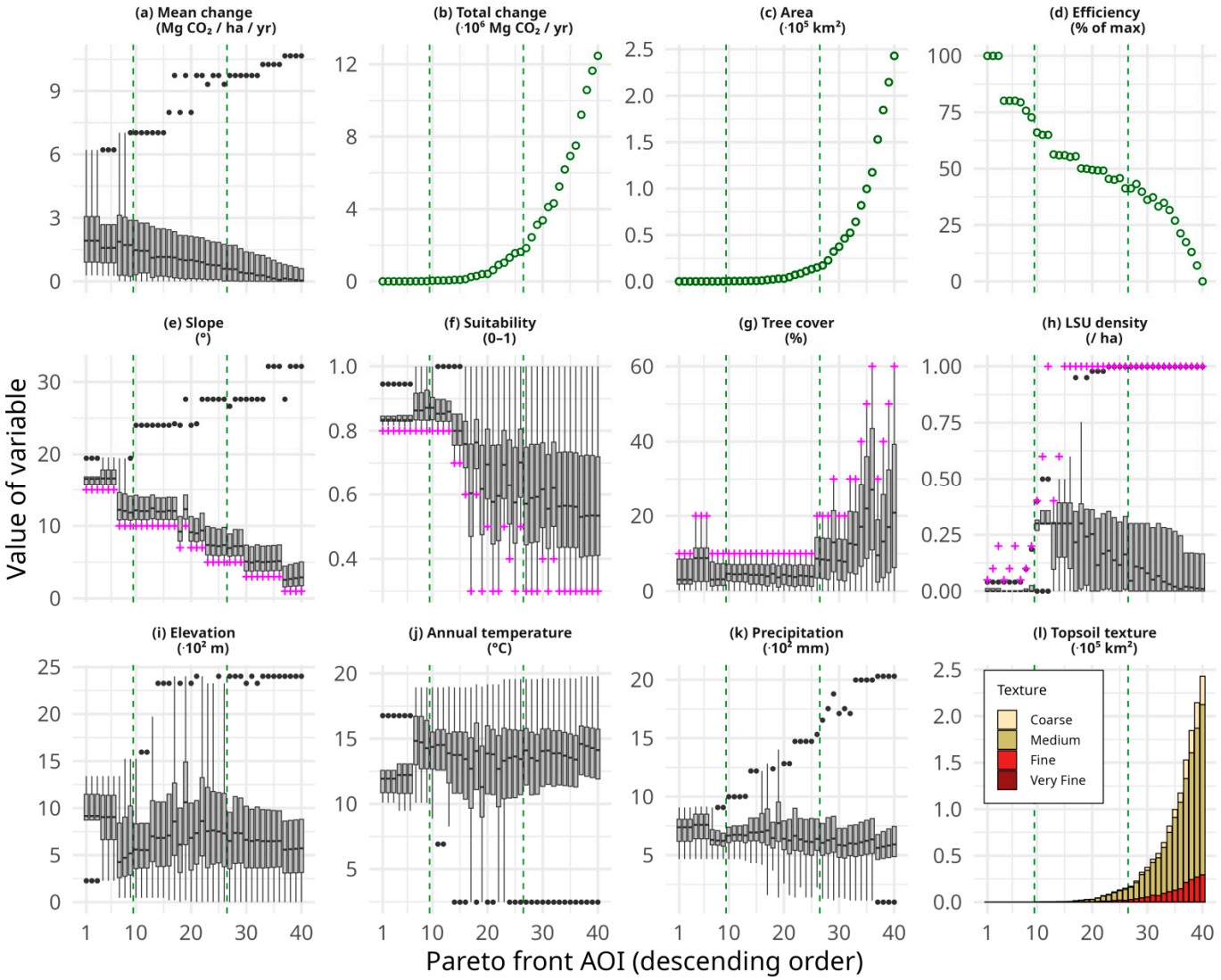

Figure 7. Environmental and threshold characteristics across Pareto-optimal scenarios. Key variables within the high-potential Areas of Interest (AOI) are shown for the 40 scenarios on the Pareto front. (**a**–**d**) Core scenario outputs: mean sequestration change, total sequestration change, total area, and efficiency score. (**e**–**h**) Applied selection thresholds: minimum slope, minimum suitability, maximum tree cover, and maximum livestock density. Crosses (+) indicate the threshold value used to define each scenario. (**i**–**l**) Environmental predictors for k-NN imputation: elevation, annual mean temperature, annual precipitation, and topsoil texture. In panels (**a**–**h**), the boxplots show the distribution of actual values within the selected AOI for each scenario; dashed vertical lines separate the three policy regimes (conservative, balanced, expansive).

Regarding the core outputs of the scenario analysis, mean sequestration change per hectare decreases with a Spearman correlation coefficient $r = -1$ against the total area and total sequestration change increases across the front, as expected (Figure 7a–c). This extreme coefficient value is by construction, as the Pareto-optimal scenarios are rank-ordered by the fundamental trade-off between efficiency and extent. The efficiency metric peaks early and then declines with a Spearman correlation $r = 1$ against mean sequestration change per hectare, confirming that the most area-efficient gains are found in the initial, more restrictive scenarios (Figure 7d).

Regarding the threshold parameters that define each scenario, the transition between regimes along the Pareto front is driven by the progressive relaxation of these selection criteria (Figure 7e–h). The conservative regime is characterised by strict thresholds, requir-

ing steeper minimum slopes and higher minimum suitability values (Figure 7e,f), while only allowing for very low maximum tree cover and livestock density (Figure 7g,h). As the strategy becomes more expansive, the thresholds for suitability and slope are relaxed, while the tolerance for higher existing tree cover and livestock density increases. Notably, the distributions of the actual environmental values within these high-potential AOI were not clustered near the threshold boundaries (point/crosses). For instance, the median slope of selected AOI was consistently much steeper than the minimum threshold required, and the actual tree cover and livestock densities were far below the maximum allowable limits (Figure 7e–h).

Regarding the rest of the environmental characteristics, the conservative scenarios on the Pareto front target localities at moderate to high elevations with lower annual temperatures and varied precipitation (Figure 7i–k). As the scenarios become more expansive, they increasingly incorporate lower-elevation, warmer, and drier areas. Topsoil texture shows a clear trend, with the initial, high-efficiency scenarios dominated by coarse and medium-textured soils, while the balanced and expansive scenarios are almost entirely composed of medium-textured soils (Figure 7l).

The land cover composition of the Pareto front AOI further clarifies these trends (Figure 8). The initial, high-efficiency scenarios primarily consist of converting shrubby and sparsely vegetated lands. The balanced regime introduces a mix of tree-covered and grassland localities. The final, expansive regime achieves its large area by including significant portions of mixed agro-systems, and existing forests and tree plantations, which contribute to the total area but offer lower marginal gains from transition.

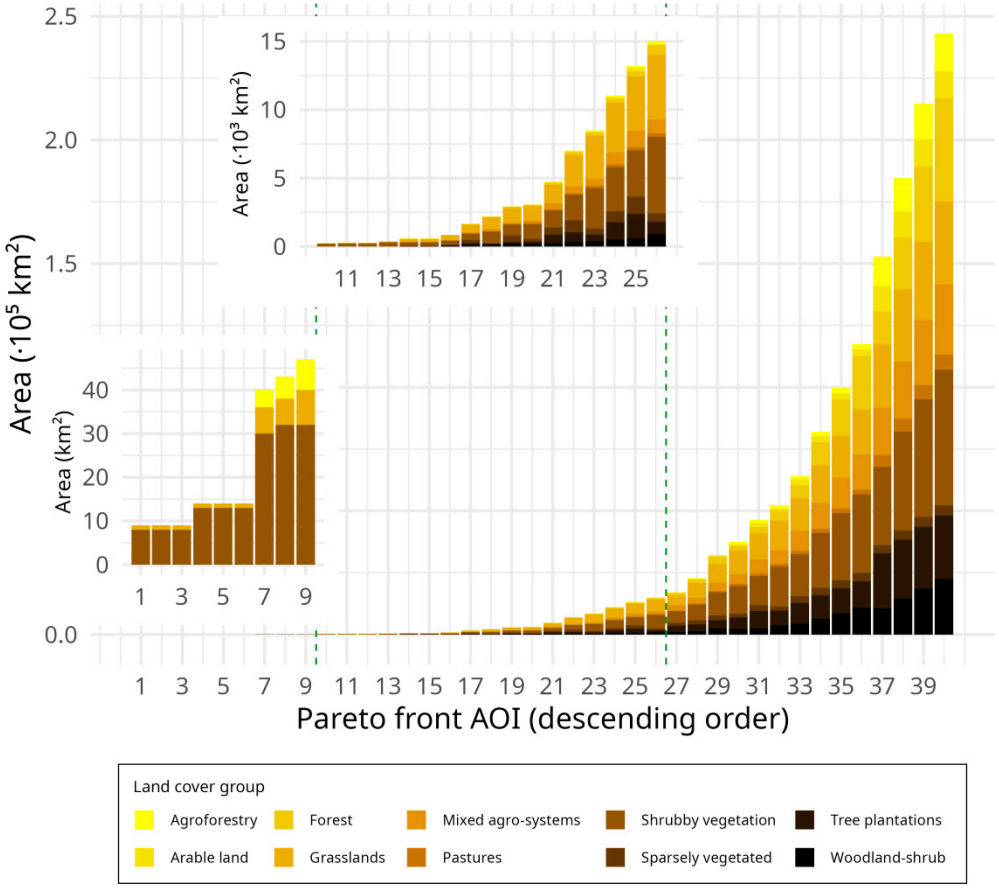

Figure 8. Area distribution of land cover groups in the high-potential areas in the scenarios of the Pareto front. The vertical lines denote change of regime. The two insets are zoomed-in versions of the first and second regime (note: *y*-axes have different scaling).

3.4. High Potential for Sequestration Change at the Administrative Level

The inter-scenario analysis reveals distinct geographic hotspots for silvopastoral implementation across the NUTS2 areas (Figure 9). The mean percentage of a NUTS2 area selected for measures was highest in central and southern Spain, in many areas of Greece, in Croatia, and in southern Italy (Figure 9a). These regions consistently appeared as high-potential across a wide range of scenarios. The spatial heterogeneity (patchiness) of selected areas within the NUTS2 areas had a negative relationship with the extent of high potential, being higher in Italy's Apulia and Liguria areas in, respectively, the south and north, in southern France, and in northern Spain (Figure 9b). This indicates that in these regions, suitable areas are fragmented. In contrast, large contiguous areas of Spain and Greece show low patchiness of high potential, suggesting that broad, landscape-scale implementation is more feasible there.

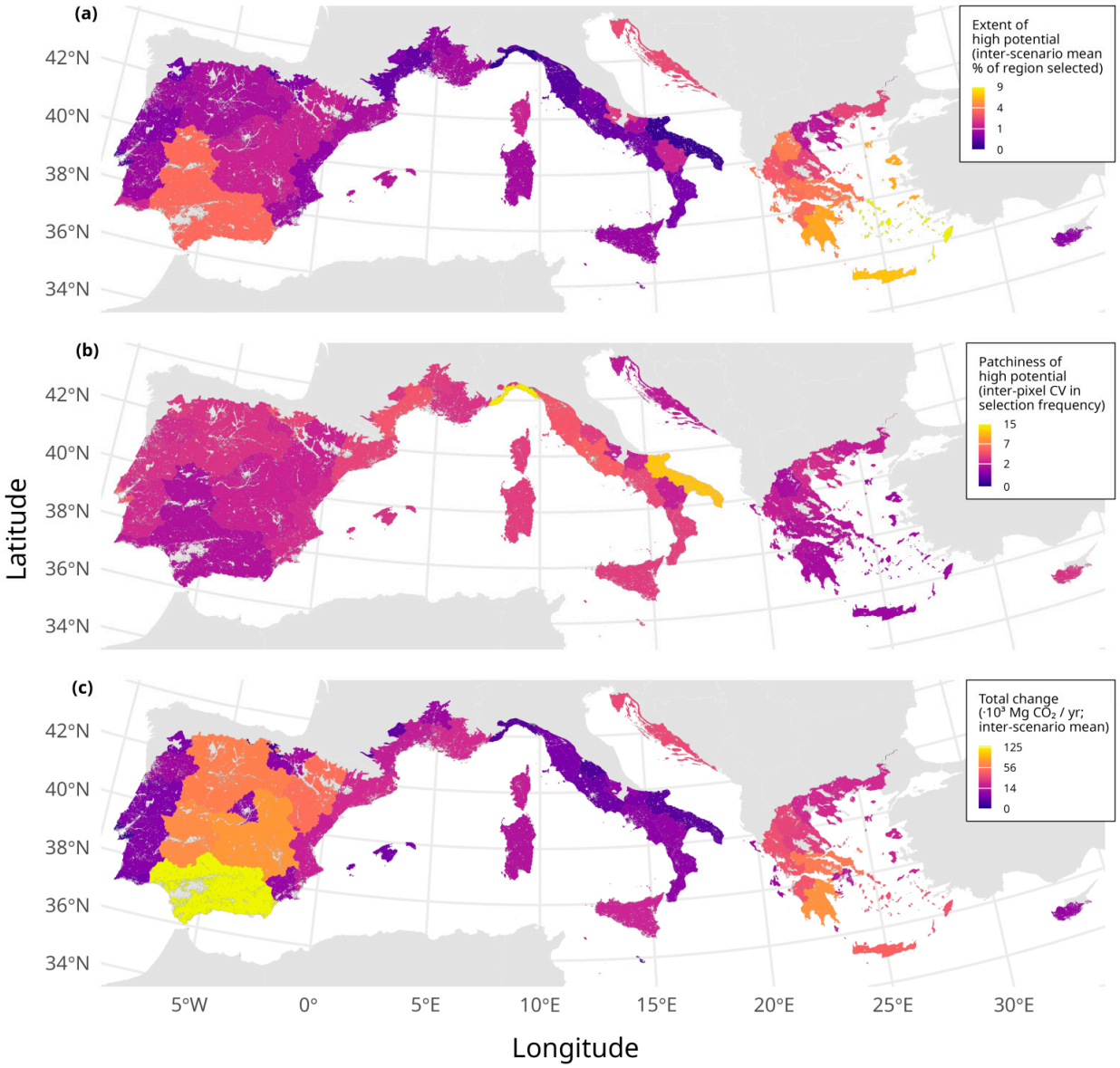

Figure 9. Potential of NUTS2 areas for being selected for silvopastoralism measures: (**a**) percent of each area's cover which was selected for measures; (**b**) spatial heterogeneity (uncertainty) of being selected for measures within each NUTS2 area, quantified as the coefficient of variation (CV) of selection frequency across all scenarios; and (**c**) total sequestration change contributed by each NUTS2 area from the baseline to the scenario measures, averaged across all 4064 scenarios.

The largest total carbon sequestration gains were concentrated in the NUTS2 regions of Andalucía, Castilla-La Mancha, and Extremadura in Spain (Figure 9c). Significant contributions are also predicted for parts of central and southern Greece, e.g., Peloponnisos (Table S6). The spatial distribution of total change at the endpoints of the Pareto front's policy regimes highlights this pattern: (1) the largest high-potential AOI of the conservative regime targets scattered hotspots in southern Spain and Greece (Figure 10a); (2) the largest high-potential AOI of the balanced regime, which was also the optimal, consolidated gains by extending from southern Spain and Greece to northern areas of these countries (Figure 10b); and (3) the largest high-potential AOI of the expansive regime broadened the implementation area across most of the Iberian Peninsula, secondarily from Greece, with moderate contributions from southern Croatia and France, as well as from Sardinia (Figure 10c).

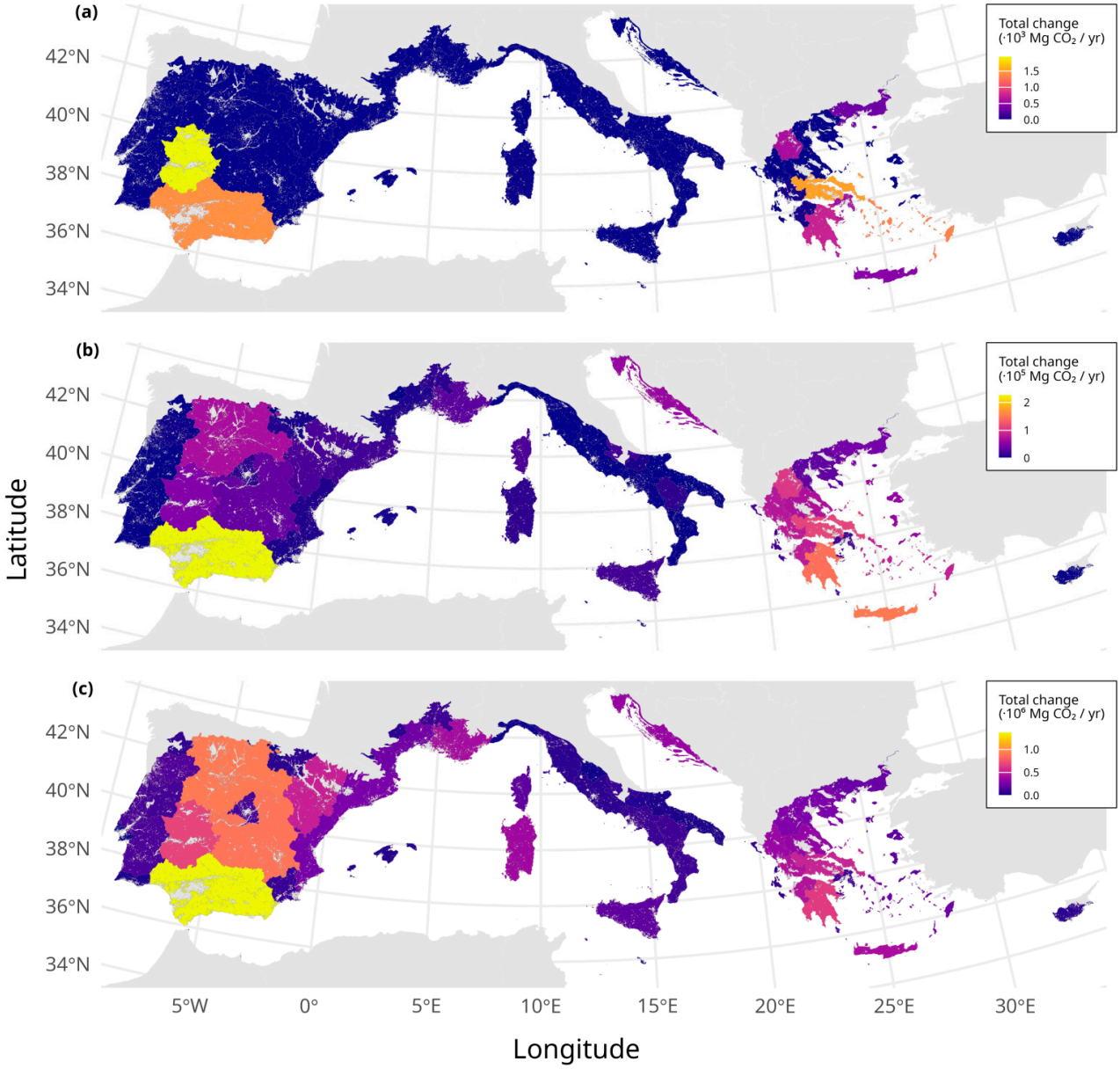

Figure 10. NUTS2 total change in carbon sequestration between the baseline and three Pareto scenarios: (**a**) the last of the conservative regime; (**b**) the last of the balanced regime, which is also the optimum Pareto point; and (**c**) the last of the expansive regime.

The analysis of the land cover groups contributing most to regional carbon gains reveals a distinct shift in the drivers of sequestration as the scenarios move from conservative to expansive (Figure 11).

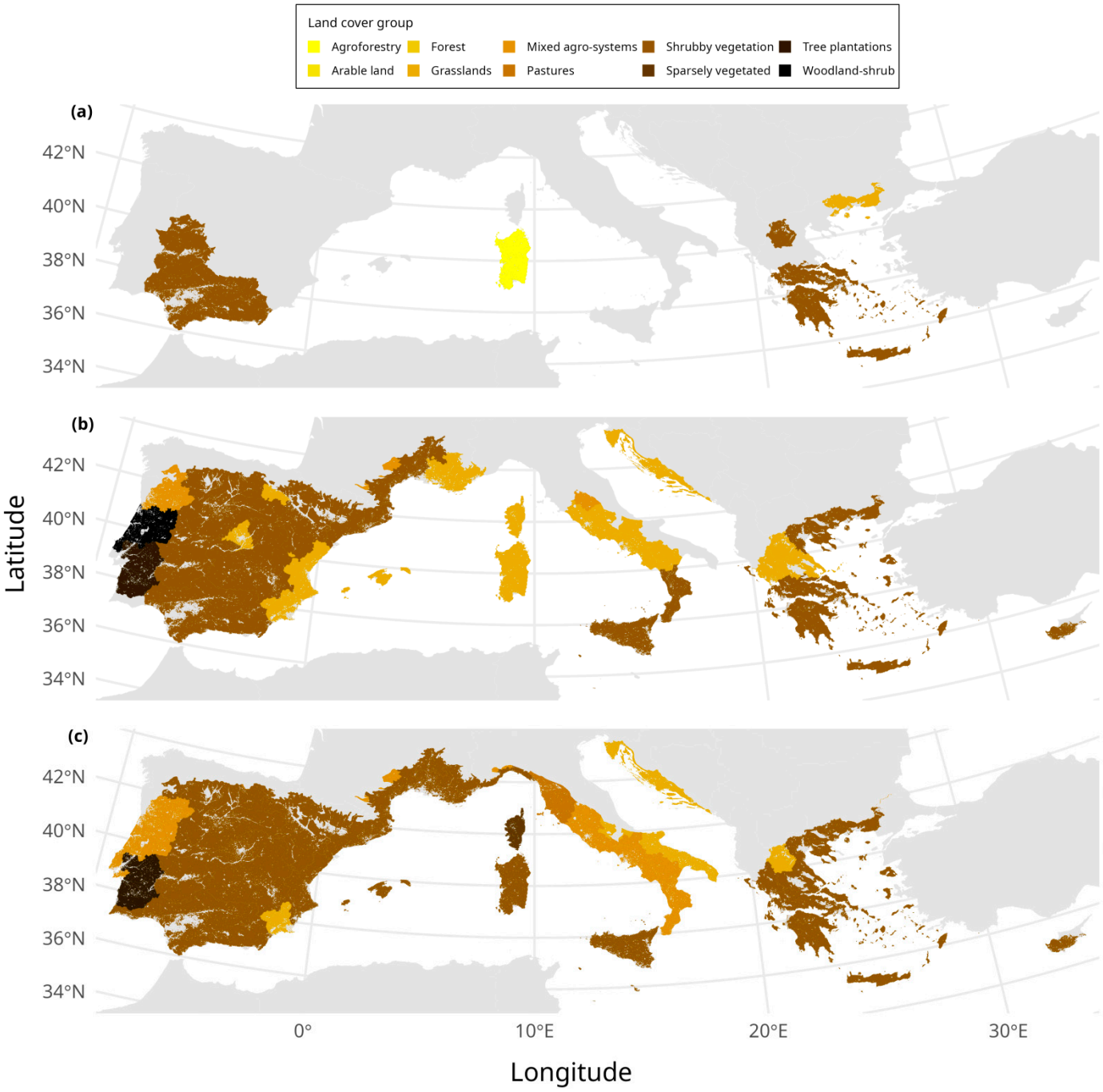

Figure 11. Dominant land cover drivers of carbon gains by policy regime. The land cover group that contributed most to total change in carbon sequestration between the baseline and three Pareto scenarios in each NUTS2 area: (**a**) the last of the conservative regime; (**b**) the last of the balanced regime, which is also the optimum Pareto point; and (**c**) the last of the expansive regime. The legend uses the consistent land cover group color palette defined in Figure 2 and Table 1.

In the conservative regime (Figure 11a), which prioritises high mean sequestration rates in small areas, the gains are almost exclusively driven by the transition of shrubby vegetation to woodland-shrub, primarily in central and southern Spain, in Greece, and the Republic of Cyprus. Under the balanced regime, which corresponds to the optimal sce-

nario (Figure 11b), the portfolio of contributing landscapes diversifies significantly. While shrubby vegetation remains a key contributor, especially in Spain and Greece, grassland transition to agroforestry emerges as another driver of sequestration gains across large territories, e.g., in the Iberian Peninsula and Italy. In the expansive regime (Figure 11c), which maximises total sequestration over the largest area, the pattern largely mirrors the balanced regime but with a broader spatial footprint. Shrubby vegetation continues to dominate as the top contributor across most of Spain, while mixed agro-systems become central to the gains in Italy, and in north/central Portugal where they take over the dominance of tree plantations in the balanced scenario. Notably, in no was the transition of arable land to agroforestry a top contributor to total change of carbon sequestration. Although arable land contributed a larger absolute area to the agroforestry transition than grasslands (Figure 3), its lower per-hectare sequestration potential resulted in it not being preferentially selected as high-potential in our scenarios.

3.5. Key Drivers of Carbon Sequestration Change

The analysis revealed that carbon sequestration potential in the Mediterranean is spatially concentrated, primarily in Spain and Greece, and is driven by the transition of marginal lands rather than prime agricultural areas. Key drivers include steep slopes (greater than 8°), low baseline tree cover (less than 30%), and minimal livestock density (less than 15 LSU ha^{-1}). The most effective strategies target shrublands and grasslands for conversion to woodland-shrub or agroforestry systems, while arable land conversion proved less impactful. A clear trade-off existed between achieving high mean sequestration rates in small, high-quality areas versus maximising total sequestration through extensive, lower-quality land incorporation.

4. Discussion

This study sought to bridge the gap between Europe's ambitious climate neutrality targets and the practical implementation of land-based mitigation strategies by developing a spatially explicit, multi-objective optimisation framework for silvopastoral expansion. Our analysis quantified the inherent trade-off between the efficiency (mean carbon gain per hectare) and the extent (total carbon gain) of silvopastoral implementation across the EU27 Mediterranean bioregion. The resulting Pareto front reveals a continuum of optimal strategies, which we categorised into three policy-relevant regimes: conservative, balanced, and expansive. These regimes provide a direct, quantitative pathway for aligning on-the-ground land-use decisions with the specific operational objectives of the EU Green Deal, such as the 2030 Climate Target Plan and the 2050 carbon neutrality goal, by offering a clear menu of options to balance immediate impact against long-term, large-scale carbon sequestration. Our findings pinpoint key geographic hotspots for implementation, primarily in the Iberian Peninsula and Greece, and demonstrate that the most efficient carbon gains are initially achieved by transitioning shrubby and sparsely vegetated lands to a mosaic of multipurpose mixed agro-systems, forests and tree plantations. This framework offers a flexible decision-support tool that allows policymakers to select strategies aligned with varying priorities, from maximising impact with limited budgets to achieving large-scale sequestration targets.

4.1. Total and Mean Carbon Sequestration Rates

The estimated annual sequestration rates in our high-potential silvopastoral areas (≈0.5–2.5 Mg CO_2 ha^{-1} $year^{-1}$, equivalent to 0.14–0.68 Mg C ha^{-1} $year^{-1}$) are consistent with the lower-to-mid range of values observed in Mediterranean agroforestry systems. Field measurements of soil and biomass carbon accumulation under olive, fruit, and mixed

tree–pasture systems generally fall between 0.35 and 1.8 Mg C ha^{-1} $year^{-1}$, depending on stand age and management intensity [91]. Meta-analyses report similarly broad variability, from modest rates of about 0.24 Mg C ha^{-1} $year^{-1}$ in older European agroforestry systems to peaks near 1.5 Mg C ha^{-1} $year^{-1}$ under improved management in Andalucian olive groves [92]. Higher values, up to 2 Mg C ha^{-1} $year^{-1}$, have been documented for almond and vineyard systems with dense cover crops, and even 5.3 Mg C ha^{-1} $year^{-1}$ where organic amendments were applied [93]. Recent research on Iberian dehesa systems aligns with this upper range, reporting total carbon stocks of 25–75 Mg C ha^{-1} and confirming the superior sequestration in wooded versus non-wooded shrublands [94]. Furthermore, a recent meta-analysis of Mediterranean carbon farming practices, including agroforestry-relevant measures like intercropping and cover crops, found an average 29% increase in soil carbon content [95].

Our higher-end mean estimates under the conservative regime reflect such a potential of transitioning degraded, low-carbon lands, where initial gains can be substantial, a phenomenon also observed in other regions where afforestation or agroforestry is established on marginal land [92]. While some studies suggest that temperate agroforestry systems can achieve even higher sequestration rates, the unique climatic stressors of the Mediterranean, such as water scarcity and high temperatures, naturally constrain productivity and carbon accumulation [96,97], a factor our spatially explicit model implicitly captures through its environmental predictors. This constraint is evidenced by recent field data from Mediterranean afforestation, which shows that young plantations may not yield a net total carbon sink for decades due to initial soil carbon losses [98]. Overall, our results align well with the conservative end of this empirical spectrum, reflecting model assumptions that exclude intensive biomass inputs and favour long-term equilibrium soil carbon accumulation.

Importantly, a portion of the projected gains, particularly in systems transitioning from open pastures, is attributable to enhanced nutrient cycling from managed livestock integration, highlighting manure's role as a valuable natural fertiliser beyond its carbon sequestration value.

4.2. Policy Implications

The identification of Spain and Greece as primary hotspots for silvopastoral expansion corroborates their long history of traditional silvopastoralism, and their significant extent of landscapes suitable for such transitions [28,35,36,99]. Our framework's preference for converting shrubby vegetation and grasslands over arable land in the most efficient scenarios is a critical finding. Many land-based mitigation strategies focus on afforesting or converting croplands, often creating conflicts with food security objectives [41,100]. Our results suggest that targeting the restoration of semi-natural shrublands and grasslands—areas often considered marginal and facing degradation or abandonment [41]—offers a more efficient pathway for initial carbon gains. The fact that arable land was never a top contributor to sequestration gains in any NUTS2 region, despite its large area, suggests that the marginal carbon benefit of converting these relatively productive soils is lower than that of restoring marginal lands.

Consequently, the primary contribution of this work is its potential to function as a decision-support tool for evidence-based policymaking. The challenge of implementing EU-level frameworks like the Green Deal, the Biodiversity Strategy, and the CAP lies in their translation to heterogeneous local contexts [1,2,101]. Our Pareto-based framework directly addresses this by making trade-offs transparent. The choice between these strategic regimes can be directly guided by the design of financial instruments like CAP eco-schemes. Policymakers can select from three strategic regimes—conservative, balanced, or expansive—depending on specific objectives and constraints. A conservative strategy,

aligned with a limited-budget CAP eco-scheme, would focus on small, targeted areas to maximise carbon gain per euro invested. An expansive strategy, suited for meeting ambitious national LULUCF targets [3], would incentivise widespread adoption to maximise total carbon sink, even at lower average efficiency. The balanced regime offers a strategic compromise, achieving a large proportion of the total potential gain with a feasible land area.

The feasibility of implementing such strategies is heightened by their alignment with existing national agricultural and forestry frameworks. For instance, Spain's "Plan Forestal" and Greece's "National Climate Law" explicitly promote agroforestry and land restoration, providing a ready policy vehicle for the conservative or balanced regimes identified here. Furthermore, growing stakeholder interest is evidenced by farmer cooperatives in Andalucía and Thessaly actively piloting silvopastoral systems supported by CAP eco-schemes, indicating a tangible demand for such spatially explicit guidance [14,39,43].

Furthermore, the aggregation of our results at the NUTS2 administrative level provides actionable insights for regional planners. The maps depicting the extent, patchiness, and total sequestration potential (Figure 9) allow for the prioritisation of entire regions for investment and policy support. For example, the vast, contiguous areas of high potential in Andalucía and Castilla-La Mancha in Spain suggest that landscape-scale programs appear well-suited, and are already supported by existing initiatives like MOSAICO [102]. In contrast, regions of high spatial heterogeneity, such as parts of southern France and northern Italy, require different approaches. The literature for such patchy Mediterranean mosaics emphasises participatory, networked strategies and farmer-to-farmer knowledge exchange, as top-down, single-measure programs are less effective [103–105].

Finally, by identifying the dominant land-cover contributor to carbon gains within each region and policy regime (Figure 11), local authorities can better tailor advisory services and incentives to local realities. This is particularly important in patchy Mediterranean mosaics where one-size-fits-all programs may perform poorly [103]. For example, our results indicate that shrubland enrichment in Greece and tree integration in Italian grasslands are key pathways. This aligns with empirical studies from Greece that call for region-specific changes like shrubland succession in marginal areas [106–108], and Italian works that favour networked, small-holder oriented interventions in mosaic grasslands [104,109]. This need for tailored approaches is underscored by a recent stakeholder analysis in Mediterranean Spain, which found that barriers vary markedly by locality (e.g., farm abandonment vs. land access issues) and that the economic viability of silvopastoralism remains a core challenge, with current policy frameworks often inadequately addressing these regional specificities [38].

While this biophysical optimisation identifies where interventions could be most effective, translating this into on-the-ground implementation requires parallel attention to socio-economic drivers. Ultimately, adoption depends on farmers' perceptions of profitability, social norms, and access to knowledge and capital [39,110].

4.3. Limitations

Despite its novel approach, our study has several limitations that must be acknowledged. First, the modelling framework relies on a static, 20-year time horizon, comparing a baseline snapshot with a future projection. Future work could integrate dynamic ecosystem models, such as the soil carbon model CENTURY, the dynamic global vegetation models LPJmL or LPJ-GUESS, or remote sensing-driven approaches like the BEPS model, to simulate carbon trajectories and feedbacks under evolving climate and management conditions [111–114]. Carbon accumulation in terrestrial ecosystems is a non-linear process that can take many decades to reach equilibrium [98]. Moreover, our use of a k-NN space-

for-time substitution to project future carbon stocks is a well-established method [115], but assumes that transitioned landscapes will eventually converge with the carbon stocks of existing analogous systems, which may not fully account for novel climatic conditions or path dependency in ecosystem development.

Second, our livestock-mediated carbon model, while based on IPCC guidelines [64], uses generalised parameters for intake and sequestration efficiency. These factors can vary significantly based on species, breed, animal age, forage availability and quality, grazing intensity, and applied systems and practices of grazing [116–118]. The model also does not account for potential negative impacts of livestock, such as soil compaction or methane emissions, which could offset some of the carbon benefits, particularly at high stocking densities [116]. Nevertheless, to minimise the aforementioned risks, we deliberately limited our simulations to a maximum stocking density of 1 LSU per hectare. This conservative threshold aligns with the need for high-resolution data to assess environmental risks, as emphasised by recent efforts to create harmonised European livestock datasets for sustainability analyses, and thereby assumes that negative contributions from high grazing intensity are limited [119–121].

Third, the scope of our optimisation is currently limited to a single objective: carbon sequestration. While this is a primary goal of climate policy, the true value of silvopastoralism lies in its multifunctionality, delivering co-benefits such as enhanced biodiversity, improved water regulation, reduced soil erosion, and increased farm resilience [39,122]. A key critique of many carbon-centric land-use models is that they can inadvertently lead to strategies that compromise other ecosystem services, for instance by promoting monoculture tree plantations [123]. Expert-based assessments of Mediterranean systems confirm that such trade-offs are inherent, revealing, for example, potential conflicts between carbon storage and other services like wildfire prevention [124]. By not including these co-benefits in the optimisation, our framework may overlook scenarios that are suboptimal for carbon alone but superior from a holistic sustainability perspective. The spatially explicit Pareto front developed here provides the foundational architecture for such a multi-objective expansion. Future iterations could incorporate additional policy targets (e.g., biodiversity scores, water quality indices) as separate axes in the optimisation, allowing decision-makers to visualise and navigate a multi-dimensional trade-off space.

Finally, our analysis is fundamentally biophysical and does not directly incorporate key socioeconomic dimensions critical to farmer decision-making, such as perceived profitability, land tenure security, or social acceptance. These factors are often the primary determinants of adoption, as highlighted by studies on agroforestry uptake in Mediterranean Europe [39], and by broader reviews of adoption drivers for sustainable land-use practices [15,110]. Recent quantitative studies consistently identify specific variables that are crucial for uptake, such as secure land tenure (a prerequisite for long-term investment), access to technical training, the influence of neighboring adopters, and farmers' perceptions of profitability and system complexity [110,125,126]. Moreover, the costs of transitioning—including labour, planting materials, and potential short-term income loss—are not included in our model, yet they constitute potential barriers for land managers. Future modeling efforts could integrate such socioeconomic data by adopting comprehensive conceptual frameworks that categorize drivers of adoption, from farm characteristics and social networks to individual perceptions and economic feasibility, into a structured system for spatial policy evaluation [126].

4.4. Future Perspectives

Building on this work, several avenues for future research could address these limitations, ranging from short-term technical improvements to long-term integrative frameworks.

As a short-term priority, the integration of dynamic ecosystem models to simulate the temporal trajectories of carbon accumulation under different transition pathways and climate change scenarios would provide a more detailed understanding of the timeline over which mitigation benefits can be realised.

A medium-term extension would involve incorporating economic variables, such as implementation and opportunity costs, to generate cost-effectiveness frontiers. This module could leverage harmonised, farm-level data from the EU's Farm Accountancy Data Network (FADN), allowing the identification of strategies that maximise carbon sequestration per euro invested, a critical metric for policy design [127].

In the longer term, the framework should be expanded into a true multi-objective tool that optimises for a suite of ecosystem services simultaneously, including biodiversity indicators, water quality, and soil health. This would help identify win-win scenarios and manage trade-offs between competing environmental goals. This envisioned extension follows a clear progression: from integrating dynamic biophysical models, to coupling them with economic data, then expanding the optimisation to multiple objectives.

Finally, coupling these spatial models with social science methodologies, such as farmer surveys and choice experiments, would help ground the scenarios in the lived realities and constraints of the rural communities expected to implement them. To encourage external validation and collaboration, core components of this modelling framework could be shared as open data and code, following the practice of other major land-use carbon assessments [114].

5. Conclusions

This study provides a robust, transparent, and scalable decision-support framework that quantifies the vast potential of silvopastoralism as a Nature-Based Solution for climate mitigation in the Mediterranean. By explicitly mapping the trade-offs between the intensity and scale of intervention, our work equips policymakers with the evidence needed to move from broad ambition to targeted, effective action. While important limitations remain, the optimisation approach presented here lays a critical foundation for developing more integrated and context-sensitive land-use policies that can help steer Europe towards its goal of climate neutrality while fostering resilient and multifunctional landscapes. More broadly, the framework demonstrates how integrating spatially explicit trade-off analysis into NbS planning can bridge the gap between global ecological ambition and local implementation. To be effective, such high-resolution spatial guidance should be paired with participatory policy design that incorporates local knowledge and stakeholder priorities, offering a replicable model for evaluating multifunctional land-use transitions worldwide.

Supplementary Materials: The following supporting information can be downloaded at: https://www.mdpi.com/article/10.3390/su18010439/s1, Table S1: Baseline land cover groups in NUTS2 areas; Figure S1: LUCAS points for the MaxEnt model; Figure S2: Corine land cover; Figure S3: Bioclimatic predictors; Figure S4: Topographic predictors; Figure S5: Topsoil predictors; Figure S6: Socioeconomic predictors; Figure S7: Predicted suitability for silvopastoralism; Figure S8: Vegetation carbon stock; Figure S9: Change in vegetation stock; Table S2: Statistics of baseline-to-projection change in vegetation stock; Figure S10: SOC stock; Figure S11: Change in SOC stock; Table S3: Statistics of baseline-to-projection change in SOC stock; Figure S12: LSU densities; Figure S13: Cattle density in relation to total LSU density; Table S4: Statistics of baseline LSU densities; Figure S14: LSU-mediated sequestration; Figure S15: Change in LSU-mediated sequestration; Table S5: Statistics

of baseline-to-projection change in LSU sequestration; Figure S16: Tree cover density; Figure S17: Protected areas; Figure S18: GAM partial effects; Table S6: Top 10 NUTS2 regions by total sequestration change.

Author Contributions: Conceptualization, D.A.K., I.K., D.F.; data curation, D.A.K.; formal analysis, D.A.K., D.F.; investigation, D.A.K., D.F.; methodology, D.A.K., D.F.; software, D.A.K.; supervision, D.F.; validation, D.A.K.; visualization, D.A.K.; writing—original draft, D.A.K.; writing—review and editing, D.A.K., I.K., D.F. All authors have read and agreed to the published version of the manuscript.

Funding: This research received no external funding.

Institutional Review Board Statement: Not applicable.

Informed Consent Statement: Not applicable.

Data Availability Statement: The original data and code presented in the study are openly available in Zenodo at https://doi.org/10.5281/zenodo.17482129 [128].

Conflicts of Interest: The authors declare no conflicts of interest.

References

1. European Commission. The European Green Deal. Available online: https://eur-lex.europa.eu/legal-content/EN/TXT/?uri=CELEX:52019DC0640 (accessed on 12 October 2025).
2. European Commission. EU Biodiversity Strategy for 2030—Bringing Nature Back into Our Lives. Available online: https://eur-lex.europa.eu/legal-content/EN/TXT/?uri=CELEX:52020DC0380 (accessed on 12 October 2025).
3. European Parliament & Council of the European Union Official Journal of the European Union. *Regulation (EU) 2018/841 on the Inclusion of Greenhouse Gas Emissions and Removals from Land Use, Land Use Change and Forestry (LULUCF) in the 2030 Climate and Energy Framework, and Amending Regulation (EU) No 525/2013 and Decision No 529/2013/EU; L 156, 19.6.2018*; European Environment Agency: Copenhagen, Denmark, 2018; pp. 1–25.
4. European Environment Agency. Enhancing Europe's Land Carbon Sink: Status and Prospects. Available online: https://data.europa.eu/doi/10.2800/2836317 (accessed on 12 October 2025).
5. Smith, P.; Bustamante, M.; Ahammad, H.; Clark, H.; Dong, H.; Elsiddig, E.A.; Haberl, H.; Harper, R.; House, J.; Jafari, M.; et al. Agriculture, Forestry and Other Land Use (AFOLU). In *Climate Change 2014: Mitigation of Climate Change. Contribution of Working Group III to the Fifth Assessment Report of the Intergovernmental Panel on Climate Change*; Edenhofer, O., Pichs-Madruga, R., Sokona, Y., Farahani, E., Kadner, S., Seyboth, K., Adler, A., Baum, I., Brunner, S., Eickemeier, P., et al., Eds.; Cambridge University Press: Cambridge, UK; New York, NY, USA, 2014; pp. 811–922.
6. Smith, P.; Calvin, K.; Nkem, J.; Campbell, D.; Cherubini, F.; Grassi, G.; Korotkov, V.; Le Hoang, A.; Lwasa, S.; McElwee, P.; et al. Which Practices Co-deliver Food Security, Climate Change Mitigation and Adaptation, and Combat Land Degradation and Desertification? *Glob. Change Biol.* **2020**, *26*, 1532–1575. [CrossRef]
7. Jose, S. Agroforestry for Ecosystem Services and Environmental Benefits: An Overview. *Agrofor. Syst.* **2009**, *76*, 1–10. [CrossRef]
8. Nair, P.K.R. Agroforestry Systems and Environmental Quality: Introduction. *J. Environ. Qual.* **2011**, *40*, 784–790. [CrossRef] [PubMed]
9. Montagnini, F.; Nair, P.K.R. Carbon Sequestration: An Underexploited Environmental Benefit of Agroforestry Systems. *Agrofor. Syst.* **2004**, *61–62*, 281–295. [CrossRef]
10. Kumar, B.M.; Nair, P.K.R. The Enigma of Tropical Homegardens. In *New Vistas in Agroforestry*; Nair, P.K.R., Rao, M.R., Buck, L.E., Eds.; Advances in Agroforestry; Springer: Dordrecht, The Netherlands, 2004; Volume 1, pp. 135–152. ISBN 978-90-481-6673-2.
11. De Stefano, A.; Jacobson, M.G. Soil Carbon Sequestration in Agroforestry Systems: A Meta-Analysis. *Agrofor. Syst.* **2018**, *92*, 285–299. [CrossRef]
12. Cardinael, R.; Guenet, B.; Chevallier, T.; Dupraz, C.; Cozzi, T.; Chenu, C. High Organic Inputs Explain Shallow and Deep SOC Storage in a Long-Term Agroforestry System—Combining Experimental and Modeling Approaches. *Biogeosciences* **2018**, *15*, 297–317. [CrossRef]
13. Plieninger, T.; Höchtl, F.; Spek, T. Traditional Land-Use and Nature Conservation in European Rural Landscapes. *Environ. Sci. Policy* **2006**, *9*, 317–321. [CrossRef]
14. Mosquera-Losada, M.R.; Santos, M.G.S.; Gonçalves, B.; Ferreiro-Domínguez, N.; Castro, M.; Rigueiro-Rodríguez, A.; González-Hernández, M.P.; Fernández-Lorenzo, J.L.; Romero-Franco, R.; Aldrey-Vázquez, J.A.; et al. Policy Challenges for Agroforestry Implementation in Europe. *Front. For. Glob. Chang.* **2023**, *6*, 1127601. [CrossRef]

15. Tranchina, M.; Reubens, B.; Frey, M.; Mele, M.; Mantino, A. What Challenges Impede the Adoption of Agroforestry Practices? A Global Perspective through a Systematic Literature Review. *Agrofor. Syst.* **2024**, *98*, 1817–1837. [CrossRef]
16. European Commission. Eco-Schemes. Available online: https://agriculture.ec.europa.eu/common-agricultural-policy/income-support/eco-schemes_en (accessed on 12 October 2025).
17. Schwartz, M.W.; Cook, C.N.; Pressey, R.L.; Pullin, A.S.; Runge, M.C.; Salafsky, N.; Sutherland, W.J.; Williamson, M.A. Decision Support Frameworks and Tools for Conservation. *Conserv. Lett.* **2018**, *11*, e12385. [CrossRef]
18. Castle, S.E.; Miller, D.C.; Merten, N.; Ordonez, P.J.; Baylis, K. Evidence for the Impacts of Agroforestry on Ecosystem Services and Human Well-Being in High-Income Countries: A Systematic Map. *Environ. Evid.* **2022**, *11*, 10. [CrossRef] [PubMed]
19. Loughran, T.F.; Ziehn, T.; Law, R.; Canadell, J.G.; Pongratz, J.; Liddicoat, S.; Hajima, T.; Ito, A.; Lawrence, D.M.; Arora, V.K. Limited Mitigation Potential of Forestation Under a High Emissions Scenario: Results from Multi-Model and Single Model Ensembles. *J. Geophys. Res. Biogeosci.* **2023**, *128*, e2023JG007605. [CrossRef]
20. Cheng, Y.; Lawrence, D.M.; Pan, M.; Zhang, B.; Graham, N.T.; Lawrence, P.J.; Liu, Z.; He, X. A Bioenergy-Focused versus a Reforestation-Focused Mitigation Pathway Yields Disparate Carbon Storage and Climate Responses. *Proc. Natl. Acad. Sci. USA* **2024**, *121*, e2306775121. [CrossRef]
21. De Mendonça, G.C.; Da Costa, L.M.; Abdo, M.T.V.N.; Costa, R.C.A.; Parras, R.; De Oliveira, L.C.M.; Pissarra, T.C.T.; Pacheco, F.A.L. Multicriteria Spatial Model to Prioritize Degraded Areas for Landscape Restoration through Agroforestry. *MethodsX* **2023**, *10*, 102052. [CrossRef]
22. Stewart, S.; O'Grady, A.; Mendham, D.; Smith, G.; Smethurst, P. Digital Tools for Quantifying the Natural Capital Benefits of Agroforestry: A Review. *Land* **2022**, *11*, 1668. [CrossRef]
23. Hua, F.; Liu, M.; Wang, Z. Integrating Forest Restoration into Land-Use Planning at Large Spatial Scales. *Curr. Biol.* **2024**, *34*, R452–R472. [CrossRef]
24. Ball, I.R.; Possingham, H.P.; Watts, M.E. Marxan and Relatives: Software for Spatial Conservation Prioritization. In *Spatial Conservation Prioritization*; Moilanen, A., Wilson, K.A., Possingham, H.P., Eds.; Oxford University Press: Oxford, UK, 2009; pp. 185–195. ISBN 978-0-19-954776-0.
25. Lehtomäki, J.; Moilanen, A. Methods and Workflow for Spatial Conservation Prioritization Using Zonation. *Environ. Model. Softw.* **2013**, *47*, 128–137. [CrossRef]
26. Sicuaio, T.; Zhao, P.; Pilesjo, P.; Shindyapin, A.; Mansourian, A. Sustainable and Resilient Land Use Planning: A Multi-Objective Optimization Approach. *ISPRS Int. J. Geo-Inf.* **2024**, *13*, 99. [CrossRef]
27. Warren Raffa, D.; Räsänen, T.A.; Trinchera, A.; Jouini, M.; Delin, S.; Kasparinskis, R.; Dirnēna, B.; Demir, Z.; Erdal, Ü.; Hanegraaf, M. Agricultural Decision Support Tools in Europe: What Kind of Tools Are Needed to Foster Soil Health? *Eur. J. Soil Sci.* **2025**, *76*, e70097. [CrossRef]
28. Fotakis, D.; Karmiris, I.; Kiziridis, D.A.; Astaras, C.; Papachristou, T.G. Social-Ecological Spatial Analysis of Agroforestry in the European Union with a Focus on Mediterranean Countries. *Agriculture* **2024**, *14*, 1222. [CrossRef]
29. Salvia, M.; Olazabal, M.; Fokaides, P.A.; Tardieu, L.; Simoes, S.G.; Geneletti, D.; De Gregorio Hurtado, S.; Viguié, V.; Spyridaki, N.-A.; Pietrapertosa, F.; et al. Climate Mitigation in the Mediterranean Europe: An Assessment of Regional and City-Level Plans. *J. Environ. Manag.* **2021**, *295*, 113146. [CrossRef]
30. Blondel, J.; Aronson, J. *Biology and Wildlife of the Mediterranean Region*; Oxford University Press: Oxford, UK, 2004; ISBN 978-0-19-850036-0.
31. Thompson, J.D. *Plant Evolution in the Mediterranean*; Oxford Biology; Oxford University Press: Oxford, UK, 2005; ISBN 978-0-19-851534-0.
32. MacDonald, D.; Crabtree, J.R.; Wiesinger, G.; Dax, T.; Stamou, N.; Fleury, P.; Gutierrez Lazpita, J.; Gibon, A. Agricultural Abandonment in Mountain Areas of Europe: Environmental Consequences and Policy Response. *J. Environ. Manag.* **2000**, *59*, 47–69. [CrossRef]
33. Kiziridis, D.A.; Mastrogianni, A.; Pleniou, M.; Karadimou, E.; Tsiftsis, S.; Xystrakis, F.; Tsiripidis, I. Acceleration and Relocation of Abandonment in a Mediterranean Mountainous Landscape: Drivers, Consequences, and Management Implications. *Land* **2022**, *11*, 406. [CrossRef]
34. Karmiris, I.; Papachristou, T.G.; Fotakis, D. Abandonment of Silvopastoral Practices Affects the Use of Habitats by the European Hare (*Lepus europaeus*). *Agriculture* **2022**, *12*, 678. [CrossRef]
35. Carreira, E.; Serrano, J.; Lopes De Castro, J.; Shahidian, S.; Pereira, A.F. Montado Mediterranean Ecosystem (Soil–Pasture–Tree and Animals): A Review of Monitoring Technologies and Grazing Systems. *Appl. Sci.* **2023**, *13*, 6242. [CrossRef]
36. Parra-López, C.; Sayadi, S.; Garcia-Garcia, G.; Ben Abdallah, S.; Carmona-Torres, C. Prioritising Conservation Actions towards the Sustainability of the Dehesa by Integrating the Demands of Society. *Agric. Syst.* **2023**, *206*, 103613. [CrossRef]
37. Edris, S.; Gabourel-Landaverde, V.A.; Schnabel, S.; Rubio-Delgado, J.; Olave, R. Contribution of European Agroforestry Systems to Climate Change Mitigation: Current and Future Land Use Scenarios. *Land* **2025**, *14*, 2162. [CrossRef]

38. Lecegui, A.; Olaizola, A.; Kok, K.; Varela, E. What Shapes Silvopastoralism in Mediterranean Mid-Mountain Areas? Understanding Factors, Drivers, and Dynamics Using Fuzzy Cognitive Mapping. *Ecol. Soc.* **2024**, *29*, art27. [CrossRef]
39. Varela, E.; Olaizola, A.M.; Blasco, I.; Capdevila, C.; Lecegui, A.; Casasús, I.; Bernués, A.; Martín-Collado, D. Unravelling Opportunities, Synergies, and Barriers for Enhancing Silvopastoralism in the Mediterranean. *Land Use Policy* **2022**, *118*, 106140. [CrossRef]
40. Rigueiro-Rodríguez, A.; McAdam, J.H.; Mosquera-Losada, M.R. *Agroforestry in Europe: Current Status and Future Prospects*; Advances in Agroforestry; Springer: Berlin, Germany, 2009; ISBN 978-1-4020-8271-9.
41. Roe, S.; Streck, C.; Beach, R.; Busch, J.; Chapman, M.; Daioglou, V.; Deppermann, A.; Doelman, J.; Emmet-Booth, J.; Engelmann, J.; et al. Land-based Measures to Mitigate Climate Change: Potential and Feasibility by Country. *Glob. Change Biol.* **2021**, *27*, 6025–6058. [CrossRef] [PubMed]
42. Halbac-Cotoara-Zamfir, R.; Smiraglia, D.; Quaranta, G.; Salvia, R.; Salvati, L.; Giménez-Morera, A. Land Degradation and Mitigation Policies in the Mediterranean Region: A Brief Commentary. *Sustainability* **2020**, *12*, 8313. [CrossRef]
43. Chiriacò, M.V.; Dămătîrcă, C.; Abd Alla, S.; Barilari, S.; Biancardi Aleu, R.; Brazzini, T.; Capela Lourenço, T.; De Carolis Villars, C.A.; Durand, S.; Di Lallo, G.; et al. A Catalogue of Land-Based Adaptation and Mitigation Solutions to Tackle Climate Change. *Sci. Data* **2025**, *12*, 166. [CrossRef]
44. R Core Team. R: A Language and Environment for Statistical Computing. Available online: https://www.R-project.org/ (accessed on 12 October 2025).
45. Hijmans, R.J. Terra: Spatial Data Analysis. Available online: https://CRAN.R-project.org/package=terra (accessed on 17 July 2025).
46. Hernangómez, D. Using the Tidyverse with Terra Objects: The Tidyterra Package. *J. Open Source Softw.* **2023**, *8*, 5751. [CrossRef]
47. Wickham, H. *Ggplot2: Elegant Graphics for Data Analysis*; Springer: New York, NY, USA, 2016; ISBN 978-3-319-24277-4.
48. Corine Land Cover Classes. Available online: https://land.copernicus.eu/content/corine-land-cover-nomenclature-guidelines/html/ (accessed on 1 October 2025).
49. Biogeographical Regions. Available online: https://www.eea.europa.eu/en/datahub/datahubitem-view/11db8d14-f167-4cd5-9205-95638dfd9618 (accessed on 1 October 2025).
50. CORINE Land Cover 2018 (Vector/Raster 100 m), Europe, 6-Yearly. Available online: https://land.copernicus.eu/en/products/corine-land-cover/clc2018 (accessed on 1 October 2025).
51. Merow, C.; Smith, M.J.; Silander, J.A. A Practical Guide to MaxEnt for Modeling Species' Distributions: What It Does, and Why Inputs and Settings Matter. *Ecography* **2013**, *36*, 1058–1069. [CrossRef]
52. European Commission; Statistical Office of the European Union; Publications Office. *New LUCAS 2022 Sample and Subsamples Design: Criticalities and Solutions*, 2022nd ed.; Publications Office of the European Union: Luxembourg, 2022.
53. Eurostat. LUCAS 2022: Data for All Countries. Available online: https://ec.europa.eu/eurostat/web/lucas/database/2022 (accessed on 4 October 2025).
54. Elith, J.; Phillips, S.J.; Hastie, T.; Dudík, M.; Chee, Y.E.; Yates, C.J. A Statistical Explanation of MaxEnt for Ecologists: Statistical Explanation of MaxEnt. *Divers. Distrib.* **2011**, *17*, 43–57. [CrossRef]
55. Den Herder, M.; Moreno, G.; Mosquera-Losada, R.M.; Palma, J.H.N.; Sidiropoulou, A.; Santiago Freijanes, J.J.; Crous-Duran, J.; Paulo, J.A.; Tomé, M.; Pantera, A.; et al. Current Extent and Stratification of Agroforestry in the European Union. *Agric. Ecosyst. Environ.* **2017**, *241*, 121–132. [CrossRef]
56. Fick, S.E.; Hijmans, R.J. WorldClim 2: New 1-km Spatial Resolution Climate Surfaces for Global Land Areas. *Int. J. Climatol.* **2017**, *37*, 4302–4315. [CrossRef]
57. Neteler, M.; Haas, J.; Metz, M. Copernicus Digital Elevation Model (DEM) for Europe at 100 Meter Resolution (EU-LAEA) Derived from Copernicus Global 30 Meter DEM Dataset. Available online: https://data.europa.eu/data/datasets/74d0e58f-9f51-444e-a5a7-eff4c20f05b1 1?locale=en (accessed on 12 October 2025).
58. Panagos, P.; Van Liedekerke, M.; Jones, A.; Montanarella, L. European Soil Data Centre: Response to European Policy Support and Public Data Requirements. *Land Use Policy* **2012**, *29*, 329–338. [CrossRef]
59. Eurostat. Population Structure Indicators by NUTS 3 Region. Available online: https://ec.europa.eu/eurostat/databrowser/product/page/DEMO_R_PJANIND3 (accessed on 4 October 2025).
60. Eurostat. Population Density by NUTS 3 Region. Available online: https://ec.europa.eu/eurostat/databrowser/product/page/DEMO_R_D3DENS (accessed on 4 October 2025).
61. Eurostat. Population on 1 January by Age Group, Sex and NUTS 3 Region. Available online: https://ec.europa.eu/eurostat/databrowser/product/page/DEMO_R_PJANGRP3 (accessed on 4 October 2025).
62. Eurostat. Emploi (Milliers de Personnes) Par Région NUTS 3. Available online: https://ec.europa.eu/eurostat/databrowser/product/page/NAMA_10R_3EMPERS (accessed on 4 October 2025).

63. Muscarella, R.; Galante, P.J.; Soley-Guardia, M.; Boria, R.A.; Kass, J.M.; Uriarte, M.; Anderson, R.P. ENMeval: An R Package for Conducting Spatially Independent Evaluations and Estimating Optimal Model Complexity for MaxEnt Ecological Niche Models. *Methods Ecol. Evol.* **2014**, *5*, 1198–1205. [CrossRef]
64. Dong, H.; Mangino, J.; McAllister, T.A.; Hatfield, J.L.; Johnson, D.E.; Lassey, K.R.; Aparecida de Lima, M.; Romanovskaya, A. Emissions from Livestock and Manure Management. In *2006 IPCC Guidelines for National Greenhouse Gas Inventories. Volume 4: Agriculture, Forestry and Other Land Use*; Eggleston, H.S., Buendia, L., Miwa, K., Ngara, T., Tanabe, K., Eds.; Institute for Global Environmental Strategies (IGES): Hayama, Japan, 2006; pp. 10.1–10.87.
65. Tadese, S.; Soromessa, T.; Aneseye, A.B.; Gebeyehu, G.; Noszczyk, T.; Kindu, M. The Impact of Land Cover Change on the Carbon Stock of Moist Afromontane Forests in the Majang Forest Biosphere Reserve. *Carbon Balance Manag.* **2023**, *18*, 24. [CrossRef]
66. Bulckaen, A.; Crespo, R. Vegetation Carbon Stock 2001–2020. Available online: https://data.integratedmodelling.org/dataset/global-vegetation-carbon-stock-2001-2020 (accessed on 4 October 2025).
67. Poggio, L.; de Sousa, L.M.; Batjes, N.H.; Heuvelink, G.B.M.; Kempen, B.; Ribeiro, E.; Rossiter, D. SoilGrids 2.0: Producing Soil Information for the Globe with Quantified Spatial Uncertainty. *Soil* **2021**, *7*, 217–240. [CrossRef]
68. Malek, Ž.; Romanchuk, Z.; Yashschun, O.; See, L. Spatial Distribution of Cattle, Sheep and Goat Density, and Grazed Areas for the European Union and the United Kingdom [Zenodo Data Set]. Available online: https://zenodo.org/records/13734518 (accessed on 12 October 2025).
69. Malek, Ž.; Romanchuk, Z.; Yaschun, O.; Jones, G.; Petersen, J.-E.; Fritz, S.; See, L. Improving the Representation of Cattle Grazing Patterns in the European Union. *Environ. Res. Lett.* **2024**, *19*, 114077. [CrossRef]
70. Ma, S.; He, F.; Tian, D.; Zou, D.; Yan, Z.; Yang, Y.; Zhou, T.; Huang, K.; Shen, H.; Fang, J. Variations and Determinants of Carbon Content in Plants: A Global Synthesis. *Biogeosciences* **2018**, *15*, 693–702. [CrossRef]
71. Menendez, H.M.; Brennan, J.R.; Ehlert, K.A.; Parsons, I.L. Improving Dry Matter Intake Estimates Using Precision Body Weight on Cattle Grazed on Extensive Rangelands. *Animals* **2023**, *13*, 3844. [CrossRef]
72. Primary Industries Standing Committee. *Nutrient Requirements of Domesticated Ruminants*; CSIRO Publishing: Clayton, Australia, 2007; ISBN 978-0-643-09510-6.
73. Rashid, M.; Aboshady, H.M.; Agamy, R.; Archimede, H. Milk Production and Composition in Warm-Climate Regions: A Systematic Review and Meta-Analysis. *Trop. Anim. Health Prod.* **2024**, *56*, 382. [CrossRef]
74. Ferro, M.M.; Tedeschi, L.O.; Atzori, A.S. The Comparison of the Lactation and Milk Yield and Composition of Selected Breeds of Sheep and Goats. *Transl. Anim. Sci.* **2017**, *1*, 498–506. [CrossRef] [PubMed]
75. Abdulwahid Jaber Al-Fayad, M. Evaluation of Different Chemical and Physical Components of Milk in Cows, Buffalos, Sheep, and Goats. *Arch. Razi Inst.* **2022**, *77*, 477–481. [CrossRef]
76. Osoro, K.; Ferreira, L.M.M.; García, U.; Martínez, A.; Celaya, R. Forage Intake, Digestibility and Performance of Cattle, Horses, Sheep and Goats Grazing Together on an Improved Heathland. *Anim. Prod. Sci.* **2017**, *57*, 102. [CrossRef]
77. Hanna, S.S. Estimation of Carcass Composition of Sheep, Goats and Cattle by the Urea Dilution Technique. *Pak. J. Nutr.* **2010**, *9*, 1107–1112. [CrossRef]
78. Kleiber, M. Body Size and Metabolic Rate. *Physiol. Rev.* **1947**, *27*, 511–541. [CrossRef] [PubMed]
79. Blaxter, K.L. *The Energy Metabolism of Ruminants*; Hutchinson Scientific and Technical: London, UK, 1962.
80. Johnson, K.A.; Johnson, D.E. Methane Emissions from Cattle. *J. Anim. Sci.* **1995**, *73*, 2483–2492. [CrossRef]
81. Maillard, É.; Angers, D.A. Animal Manure Application and Soil Organic Carbon Stocks: A Meta-analysis. *Glob. Change Biol.* **2014**, *20*, 666–679. [CrossRef] [PubMed]
82. Thomsen, I.K.; Christensen, B.T. Carbon Sequestration in Soils with Annual Inputs of Maize Biomass and Maize-Derived Animal Manure: Evidence from 13C Abundance. *Soil Biol. Biochem.* **2010**, *42*, 1643–1646. [CrossRef]
83. Sykes, A.J.; Topp, C.F.E.; Rees, R.M. Understanding Uncertainty in the Carbon Footprint of Beef Production. *J. Clean. Prod.* **2019**, *234*, 423–435. [CrossRef]
84. Liu, Y.; Liu, R.; Chen, J.; Wei, X.; Qi, L.; Zhao, L. A Global Annual Fractional Tree Cover Dataset during 2000–2021 Generated from Realigned MODIS Seasonal Data. *Sci. Data* **2024**, *11*, 832. [CrossRef]
85. European Environment Agency. Natura 2000 Dataset (End 2021 Revision 1). Available online: https://sdi.eea.europa.eu/data/dae737fd-7ee1-4b0a-9eb7-1954eec00c65 (accessed on 29 October 2025).
86. European Environment Agency. Common Database on Designated Areas (CDDA) V2021, Public Version. Available online: https://sdi.eea.europa.eu/data/c0c9663b-ea1c-4068-b8b5-533f40539bdf (accessed on 29 October 2025).
87. Aryal, D.R.; Morales-Ruiz, D.E.; López-Cruz, S.; Tondopó-Marroquín, C.N.; Lara-Nucamendi, A.; Jiménez-Trujillo, J.A.; Pérez-Sánchez, E.; Betanzos-Simon, J.E.; Casasola-Coto, F.; Martínez-Salinas, A.; et al. Silvopastoral Systems and Remnant Forests Enhance Carbon Storage in Livestock-Dominated Landscapes in Mexico. *Sci. Rep.* **2022**, *12*, 16769. [CrossRef]
88. Mackay-Smith, T.H.; Burkitt, L.; Reid, J.; López, I.F.; Phillips, C. A Framework for Reviewing Silvopastoralism: A New Zealand Hill Country Case Study. *Land* **2021**, *10*, 1386. [CrossRef]

89. Christopoulos, T.P. Inflection: Finds the Inflection Point of a Curve. Available online: https://CRAN.R-project.org/package=inflection (accessed on 29 October 2025).
90. Wood, S.N. Mgcv: Mixed GAM Computation Vehicle with Automatic Smoothness Estimation. Available online: https://CRAN.R-project.org/package=mgcv (accessed on 29 October 2025).
91. Funes, I.; Molowny-Horas, R.; Savé, R.; De Herralde, F.; Aranda, X.; Vayreda, J. Carbon Stocks and Changes in Biomass of Mediterranean Woody Crops over a Six-Year Period in NE Spain. *Agron. Sustain. Dev.* **2022**, *42*, 98. [CrossRef]
92. Carranca, C.; Pedra, F.; Madeira, M. Enhancing Carbon Sequestration in Mediterranean Agroforestry Systems: A Review. *Agriculture* **2022**, *12*, 1598. [CrossRef]
93. Vicente-Vicente, J.L.; García-Ruiz, R.; Francaviglia, R.; Aguilera, E.; Smith, P. Soil Carbon Sequestration Rates under Mediterranean Woody Crops Using Recommended Management Practices: A Meta-Analysis. *Agric. Ecosyst. Environ.* **2016**, *235*, 204–214. [CrossRef]
94. González-Morales, M.; Rodríguez-González, M.Á.; Paredes, D.; Fernández-Pozo, L. Influence of Mediterranean Shrublands Management on Soil Carbon Sequestration. *iScience* **2025**, *28*, 113057. [CrossRef]
95. Andrés, P.; Delgado, A.; Doblas-Miranda, E.; Berk, B. Carbon Farming, Crop Yield and Biodiversity in Mediterranean Europe: The Dose Makes the Poison? *Plant Soil* **2025**. [CrossRef]
96. Ruiz-Peinado, R.; Bravo-Oviedo, A.; López-Senespleda, E.; Bravo, F.; Del Río, M. Forest Management and Carbon Sequestration in the Mediterranean Region: A Review. *For. Syst.* **2017**, *26*, eR04S. [CrossRef]
97. Van Der Woude, A.M.; Peters, W.; Joetzjer, E.; Lafont, S.; Koren, G.; Ciais, P.; Ramonet, M.; Xu, Y.; Bastos, A.; Botía, S.; et al. Temperature Extremes of 2022 Reduced Carbon Uptake by Forests in Europe. *Nat. Commun.* **2023**, *14*, 6218. [CrossRef]
98. Renna, V.; Martín-Gallego, P.; Julián, F.; Six, J.; Cardinael, R.; Laub, M. Initial Soil Carbon Losses May Offset Decades of Biomass Carbon Accumulation in Mediterranean Afforestation. *Geoderma Reg.* **2024**, *36*, e00768. [CrossRef]
99. Papanastasis, V.P.; Mantzanas, K.; Dini-Papanastasi, O.; Ispikoudis, I. Traditional Agroforestry Systems and Their Evolution in Greece. In *Agroforestry in Europe*; Rigueiro-Rodróguez, A., McAdam, J., Mosquera-Losada, M.R., Eds.; Advances in Agroforestry; Springer: Dordrecht, The Netherlands, 2009; Volume 6, pp. 89–109. ISBN 978-1-4020-8271-9.
100. Fujimori, S.; Wu, W.; Doelman, J.; Frank, S.; Hristov, J.; Kyle, P.; Sands, R.; Van Zeist, W.-J.; Havlik, P.; Domínguez, I.P.; et al. Land-Based Climate Change Mitigation Measures Can Affect Agricultural Markets and Food Security. *Nat. Food* **2022**, *3*, 110–121. [CrossRef] [PubMed]
101. European Commission; Directorate-General for Agriculture and Rural Development; Unit A.3 (Policy Performance); European Evaluation Helpdesk for the CAP. Rough Estimate of the Climate Change Mitigation Potential of the CAP Strategic Plans (EU-27) over the 2023–2027 Period. Available online: https://eu-cap-network.ec.europa.eu/publications/rough-estimates-climate-change-mitigation-potential-cap-strategic-plans-eu-27-over_en (accessed on 12 October 2025).
102. Wolpert, F.; Quintas-Soriano, C.; Pulido, F.; Huntsinger, L.; Plieninger, T. Collaborative Agroforestry to Mitigate Wildfires in Extremadura, Spain: Land Manager Motivations and Perceptions of Outcomes, Benefits, and Policy Needs. *Agrofor. Syst.* **2022**, *96*, 1135–1149. [CrossRef]
103. Agnoletti, M.; Santoro, A. Rural Landscape Planning and Forest Management in Tuscany (Italy). *Forests* **2018**, *9*, 473. [CrossRef]
104. Bagella, S.; Caria, M.C.; Seddaiu, G.; Leites, L.; Roggero, P.P. Patchy Landscapes Support More Plant Diversity and Ecosystem Services than Wood Grasslands in Mediterranean Silvopastoral Agroforestry Systems. *Agric. Syst.* **2020**, *185*, 102945. [CrossRef]
105. Barlagne, C.; Bézard, M.; Drillet, E.; Larade, A.; Diman, J.-L.; Alexandre, G.; Vinglassalon, A.; Nijnik, M. Stakeholders' Engagement Platform to Identify Sustainable Pathways for the Development of Multi-Functional Agroforestry in Guadeloupe, French West Indies. *Agrofor. Syst.* **2023**, *97*, 463–479. [CrossRef]
106. Tsiakiris, R.; Stara, K.; Kazoglou, Y.; Kakouros, P.; Bousbouras, D.; Dimalexis, A.; Dimopoulos, P.; Fotiadis, G.; Gianniris, I.; Kokkoris, I.P.; et al. Agroforestry and the Climate Crisis: Prioritizing Biodiversity Restoration for Resilient and Productive Mediterranean Landscapes. *Forests* **2024**, *15*, 1648. [CrossRef]
107. Gemitzi, A.; Albarakat, R.; Kratouna, F.; Lakshmi, V. Land Cover and Vegetation Carbon Stock Changes in Greece: A 29-Year Assessment Based on CORINE and Landsat Land Cover Data. *Sci. Total Environ.* **2021**, *786*, 147408. [CrossRef]
108. Badalamenti, E.; Battipaglia, G.; Gristina, L.; Novara, A.; Rühl, J.; Sala, G.; Sapienza, L.; Valentini, R.; La Mantia, T. Carbon Stock Increases up to Old Growth Forest along a Secondary Succession in Mediterranean Island Ecosystems. *PLoS ONE* **2019**, *14*, e0220194. [CrossRef]
109. Facioni, L.; Burrascano, S.; Chiti, T.; Giarrizzo, E.; Zanini, M.; Blasi, C. Changes in Plant Diversity and Carbon Stocks along a Succession from Semi-Natural Grassland to Submediterranean *Quercus cerris* L. Woodland in Central Italy. *Phytocoenologia* **2019**, *49*, 393–408. [CrossRef]
110. Zabala, A.; Pascual, U.; García-Barrios, L.E.; Mukherjee, N. Drivers to Adopt Agroforestry and Sustainable Land-Use Innovations: A Review and Framework for Policy. *Land Use Policy* **2025**, *151*, 107468. [CrossRef]
111. Parton, W.J. The CENTURY Model. In *Evaluation of Soil Organic Matter Models*; Powlson, D.S., Smith, P., Smith, J.U., Eds.; Springer: Berlin/Heidelberg, Germany, 1996; pp. 283–291. ISBN 978-3-642-64692-8.

112. Schaphoff, S.; Von Bloh, W.; Rammig, A.; Thonicke, K.; Biemans, H.; Forkel, M.; Gerten, D.; Heinke, J.; Jägermeyr, J.; Knauer, J.; et al. LPJmL4—A Dynamic Global Vegetation Model with Managed Land—Part 1: Model Description. *Geosci. Model Dev.* **2018**, *11*, 1343–1375. [CrossRef]
113. Smith, B.; Wårlind, D.; Arneth, A.; Hickler, T.; Leadley, P.; Siltberg, J.; Zaehle, S. Implications of Incorporating N Cycling and N Limitations on Primary Production in an Individual-Based Dynamic Vegetation Model. *Biogeosciences* **2014**, *11*, 2027–2054. [CrossRef]
114. Peng, D.; Zhang, B.; Zheng, S.; Ju, W.; Chen, J.M.; Ciais, P.; Guo, H.; Pan, Y.; Yu, L.; Xu, Y.; et al. Newly Established Forests Dominated Global Carbon Sequestration Change Induced by Land Cover Conversions. *Nat. Commun.* **2025**, *16*, 6570. [CrossRef] [PubMed]
115. Suchenwirth, L.; Stümer, W.; Schmidt, T.; Förster, M.; Kleinschmit, B. Large-Scale Mapping of Carbon Stocks in Riparian Forests with Self-Organizing Maps and the k-Nearest-Neighbor Algorithm. *Forests* **2014**, *5*, 1635–1652. [CrossRef]
116. Purcell, M.; DuPont, J.; Somenahally, A.; McLawrence, J.F.; Case, C.L.; Gowda, P.; King, N.; Rouquette, M., Jr.; Yu, R.-Q. Long-Term Grazing and Nitrogen Management Impacted Methane Emission Potential and Soil Microbial Community in Grazing Pastures. *Environ. Health* **2025**, *3*, 68–78. [CrossRef] [PubMed]
117. Smith, W.B.; Galyean, M.L.; Kallenbach, R.L.; Greenwood, P.L.; Scholljegerdes, E.J. Understanding Intake on Pastures: How, Why, and a Way Forward. *J. Anim. Sci.* **2021**, *99*, skab062. [CrossRef]
118. Shilpakar, C.; Yang, D.; Holbrook, D.L.; Norton, U.; Islam, M.A. Impact of Grazing Duration and Environment on Soil Carbon in Reclaimed Uranium Mines Tailings: A Region Specific Study. *Land Degrad. Dev.* **2025**, *36*, 4474–4485. [CrossRef]
119. Malek, Ž.; Romanchuk, Z.; Yashchun, O.; See, L. A Harmonized Data Set of Ruminant Livestock Presence and Grazing Data for the European Union and Neighbouring Countries. *Sci. Data* **2024**, *11*, 1136. [CrossRef]
120. Milazzo, F.; Francksen, R.M.; Abdalla, M.; Ravetto Enri, S.; Zavattaro, L.; Pittarello, M.; Hejduk, S.; Newell-Price, P.; Schils, R.L.M.; Smith, P.; et al. An Overview of Permanent Grassland Grazing Management Practices and the Impacts on Principal Soil Quality Indicators. *Agronomy* **2023**, *13*, 1366. [CrossRef]
121. Patton, B.D.; Dong, X.; Nyren, P.E.; Nyren, A. Effects of Grazing Intensity, Precipitation, and Temperature on Forage Production. *Rangel. Ecol. Manag.* **2007**, *60*, 656–665. [CrossRef]
122. Amorim, H.C.S.; Ashworth, A.J.; O'Brien, P.L.; Thomas, A.L.; Runkle, B.R.K.; Philipp, D. Temperate Silvopastures Provide Greater Ecosystem Services than Conventional Pasture Systems. *Sci. Rep.* **2023**, *13*, 18658. [CrossRef] [PubMed]
123. Suarez, A.; Gwozdz, W. On the Relation between Monocultures and Ecosystem Services in the Global South: A Review. *Biol. Conserv.* **2023**, *278*, 109870. [CrossRef]
124. Lecegui, A.; Olaizola, A.M.; Varela, E. Disentangling the Role of Management Practices on Ecosystem Services Delivery in Mediterranean Silvopastoral Systems: Synergies and Trade-Offs through Expert-Based Assessment. *For. Ecol. Manag.* **2022**, *517*, 120273. [CrossRef]
125. Alvarado Sandino, C.O.; Barnes, A.P.; Sepúlveda, I.; Garratt, M.P.D.; Thompson, J.; Escobar-Tello, M.P. Examining Factors for the Adoption of Silvopastoral Agroforestry in the Colombian Amazon. *Sci. Rep.* **2023**, *13*, 12252. [CrossRef]
126. Chamorro-Vargas, C.T.; Morgan, S.; Pantevéz, H.; Gomez, M.; Kennedy, C.M.; Kremen, C. Enablers and Barriers to Adoption of Sustainable Silvopastoral Practices for Livestock Production in Colombia. *Front. Sustain. Food Syst.* **2025**, *9*, 1600091. [CrossRef]
127. Tammi, I.; Mustajärvi, K.; Rasinmäki, J. Integrating Spatial Valuation of Ecosystem Services into Regional Planning and Development. *Ecosyst. Serv.* **2017**, *26*, 329–344. [CrossRef]
128. Kiziridis, D.; Karmiris, I.; Fotakis, D. Data and Code for "Agroforestry Optimisation for Climate Policy: Mapping Silvopastoral Carbon Sequestration Trade-Offs in the Mediterranean" [Zenodo Data Set]. Available online: https://zenodo.org/records/17482130 (accessed on 29 December 2025).